MECHANICAL BEHAVIOR AND FATIGUE STUDIES OF RUBBER COMPONENTS IN ARMY TRACKED VEHICLES

H.R. Brown, J.L. Bouvard, D. Oglesby, E. Marin, D. Francis, A. Antonyraj, H. Toghiani, P. Wang, M.F. Horstemeyer, M.P. Castanier

This project was funded by SimBRS and performed at the Center for Advanced Vehicular Systems (CAVS) at MSU

GVSETS

Report Documentation Page

Form Approved
OMB No. 0704-0188

1. REPORT DATE	2. REPORT TYPE	3. DATES COVERED
13 AUG 2010	**N/A**	**-**

4. TITLE AND SUBTITLE	5a. CONTRACT NUMBER
Mechanical Behavior and Fatigue Studies of Rubber Components in Army Tracked Vehicles	5b. GRANT NUMBER **W56 HZV-08-C-0236 (SimBRS)**
	5c. PROGRAM ELEMENT NUMBER
6. AUTHOR(S) **H.R. Brown; J.L. Bouvard; D. Oglesby; E. Marin; D. Francis; A. Antonyraj; H. Toghiani; P. Wang; M.F. Horstemeyer; M.P. Castanier**	5d. PROJECT NUMBER
	5e. TASK NUMBER
	5f. WORK UNIT NUMBER
7. PERFORMING ORGANIZATION NAME(S) AND ADDRESS(ES) **The Center for Advanced Vehicular Systems (CAVS) at Michigan State University**	8. PERFORMING ORGANIZATION REPORT NUMBER
9. SPONSORING/MONITORING AGENCY NAME(S) AND ADDRESS(ES) **US Army RDECOM-TARDEC 6501 E 11 Mile Rd Warren, MI 48397-5000, USA**	10. SPONSOR/MONITOR'S ACRONYM(S) **TACOM/TARDEC**
	11. SPONSOR/MONITOR'S REPORT NUMBER(S) **21108RC**

12. DISTRIBUTION/AVAILABILITY STATEMENT
Approved for public release, distribution unlimited

13. SUPPLEMENTARY NOTES
Presented at NDIAs Ground Vehicle Systems Engineering and Technology Symposium (GVSETS), 17 22 August 2009,Troy, Michigan, USA, The original document contains color images.

14. ABSTRACT

15. SUBJECT TERMS

16. SECURITY CLASSIFICATION OF:			17. LIMITATION OF ABSTRACT	18. NUMBER OF PAGES	19a. NAME OF RESPONSIBLE PERSON
a. REPORT **unclassified**	b. ABSTRACT **unclassified**	c. THIS PAGE **unclassified**	**SAR**	**39**	

Introduction

- Monotonic approach
  - Internal state variable (ISV) model for metals
  - ISV modeling strategy moved to glassy polymers (Bouvard et al., 2010)
  - Current efforts to apply ISV modeling strategy to elastomers
- Fatigue approach
  - Researchers have historically separated fatigue crack initiation and propagation
  - (McDowell et al., 2003) refined the earlier crack stages into incubation and microstructurally and physically small crack growth, greatly increasing accuracy
  - Microstructure has been incorporated into the multistage modeling for metals at CAVS
  - Researchers have typically only investigated long crack for elastomers (Mars and Fatemi, 2003; Busfield et al., 2002; Chou et al., 2007)
  - Current efforts are to add MSC/PSC, INC to fatigue modeling of elastomers and incorporate microstructure

Overview

Experiments and Stereology to Capture Structure–Property Relationships

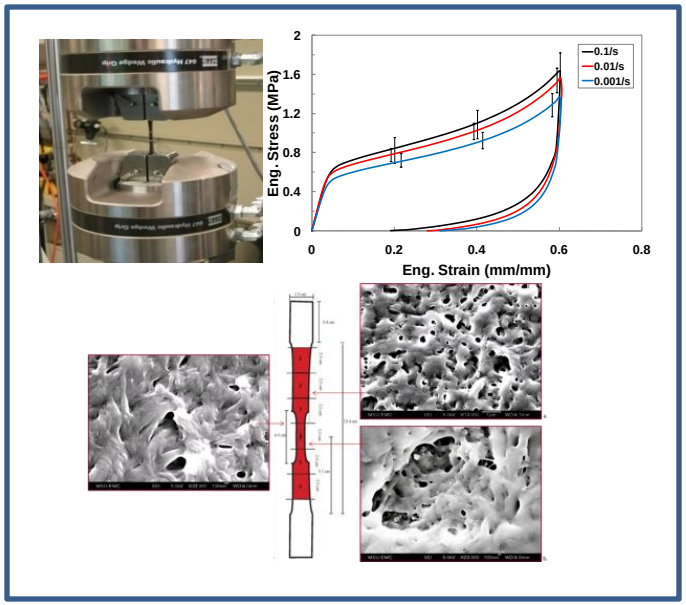

Multi-Scale Internal State Variable Modeling

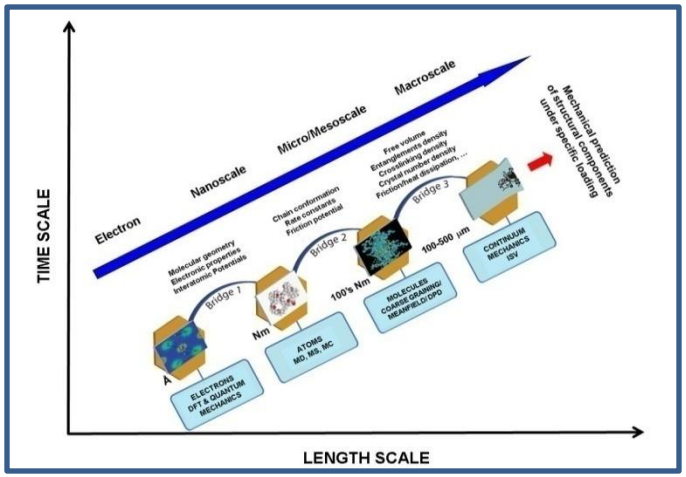

Material Database and FEA Material Model Development for Polymer Materials

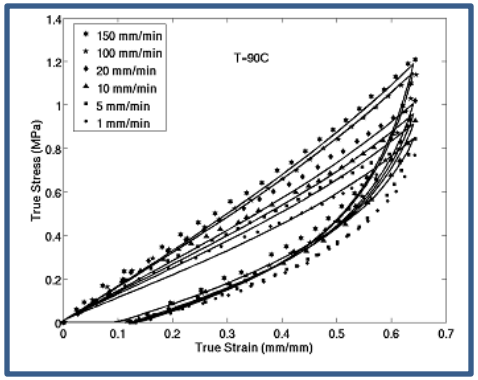

Model Verification at Material Level

System Level Modeling

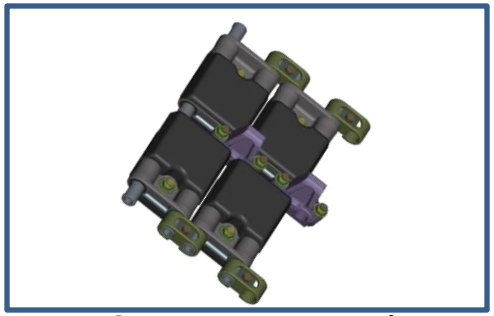

Component Level Validation

Motivation

- Components of focus on tank track
  - Bushings
  - Road wheels
  - Suspension
  - Backer pads
- Extreme Loading conditions
  - High temperature
  - High friction
  - Complex loading
- Road wheel backer pad failure at one-half of the design target mileage

Macroscale MSU ISV/MSF Models Implementation and Use

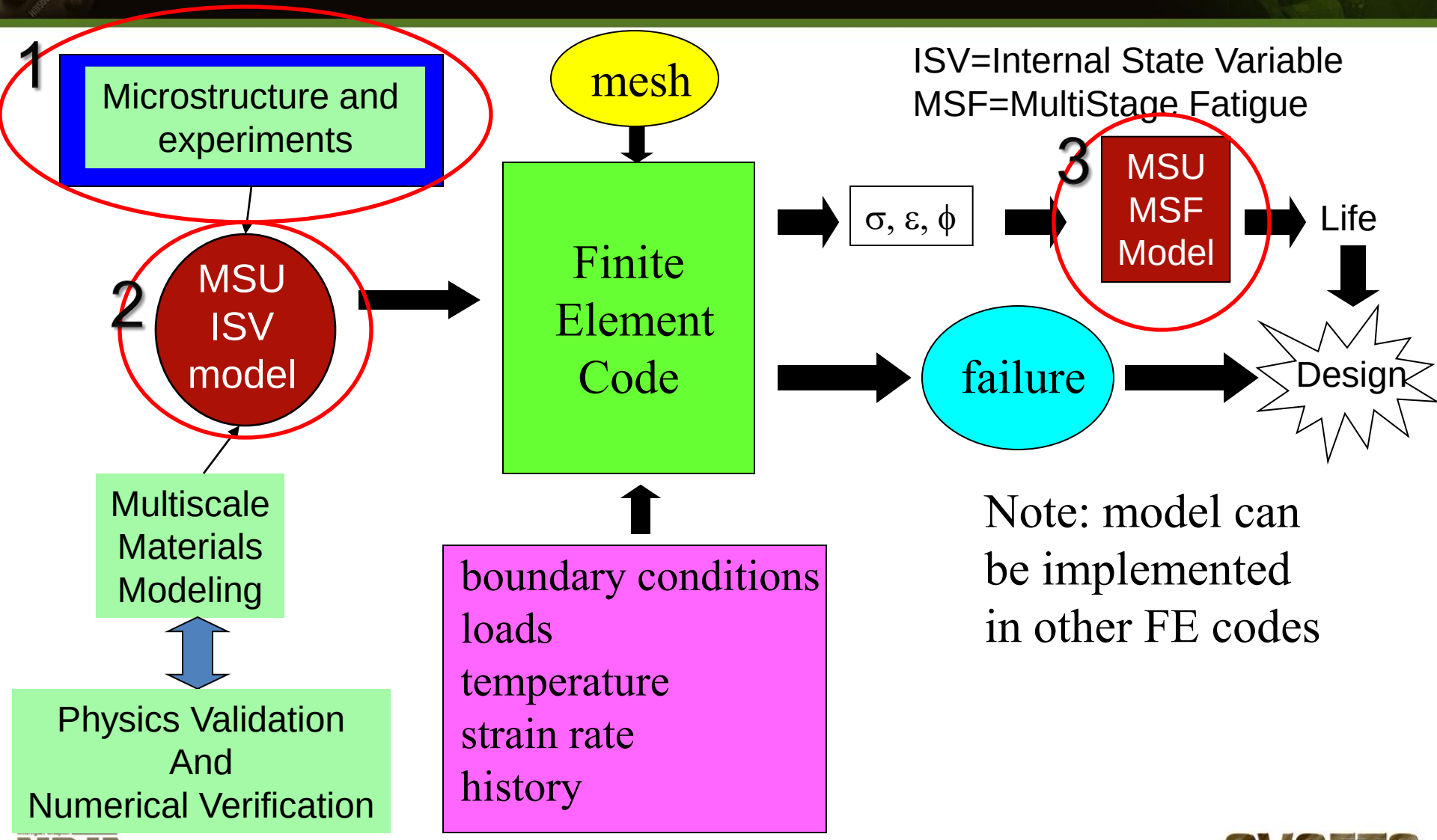

Multiscale Experiments

1. Exploratory exps
2. Model correlation exps
3. Model validation exps

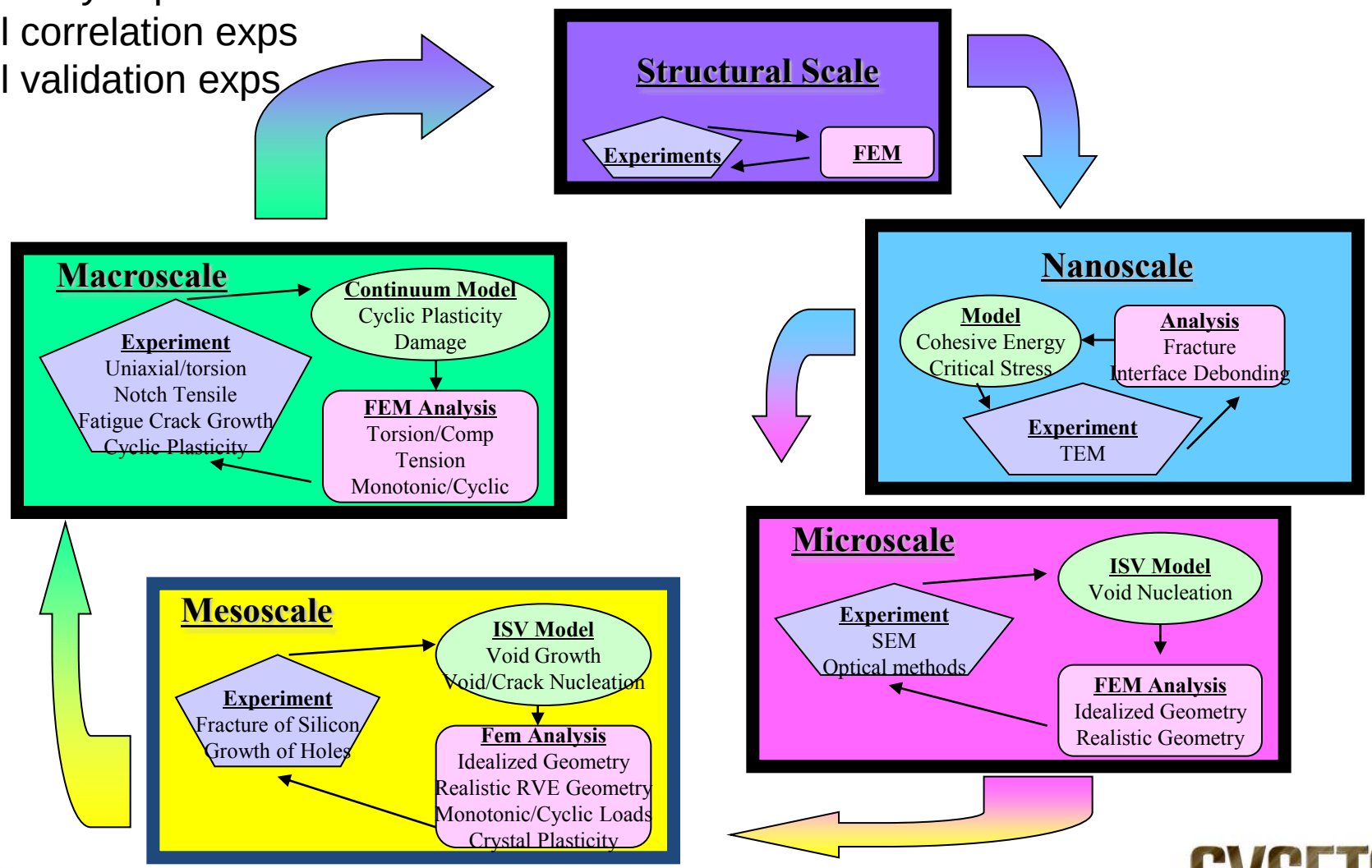

Material: Styrene Butadiene Rubber

- Random copolymer – styrene and butadiene are randomly distributed throughout the polymer chain
- 3:1 butadiene to styrene by weight
- Commercially used in a wide range of projects

General properties of SBR

Property	Value	Units
Glass Transition temperature	-40	° C
Temperature range	-28 to 76	° C
Tensile strength	4.8	MPa
Stretch Limit	150	%
Density	91.5	Lbs/cu ft

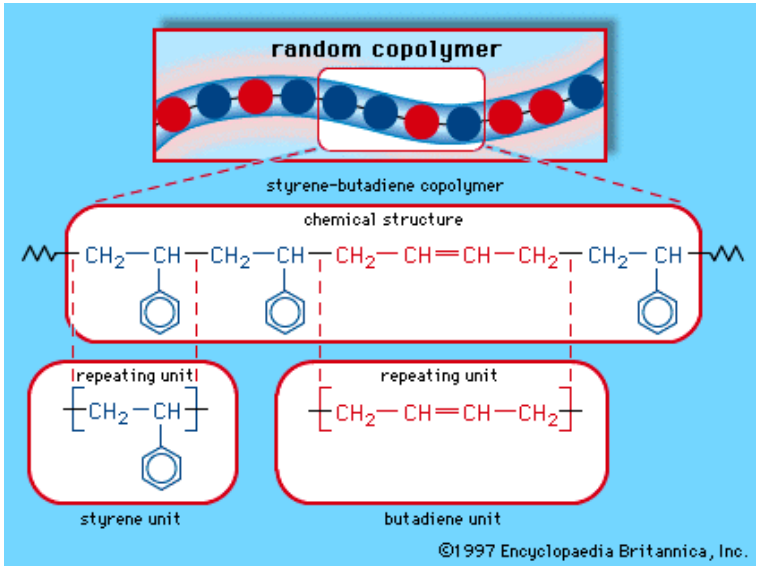

Experimental Methods: DMA

- Dynamic mechanical analysis
  - TA Instrument Q900 Dynamic Mechanical Analyzer
  - Rectangular 1.5 in x 0.135 in x 0.06 in specimen with DMA tensile clamps (ASTM D4065-01)
  - Oscillated at 1 Hz for a range of temperatures to include temperature transitions
  - Tg measured using midpoint method

Experimental Methods: Set-up

Compression Test

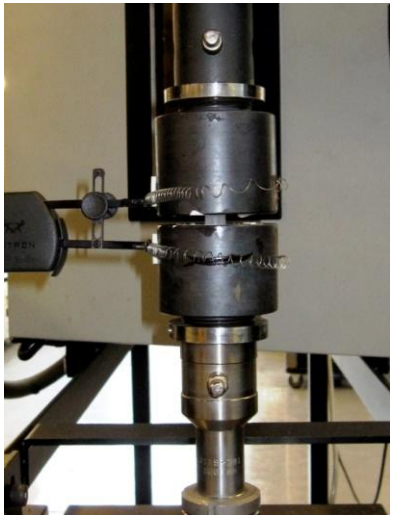

Low strain rates
(10^{-4} s^{-1} to 10^{-1} s^{-1})

Hopkinson Bar

High strain rates
(1200 s^{-1} to 3000 s^{-1})

Tension Test

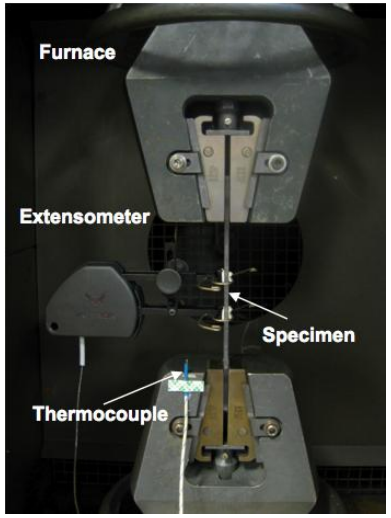

Low strain rates
(10^{-4} s^{-1} to 10^{-1} s^{-1})

Fatigue Test

Low frequency
(2Hz)

Specimen Geometry

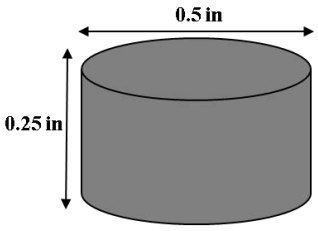

Geometry of 0.5 L/D ratio

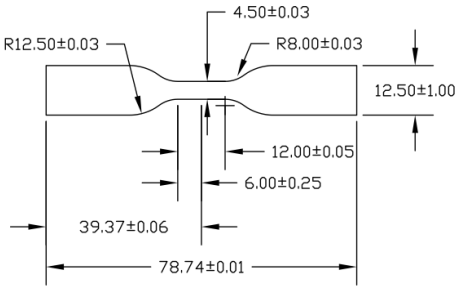

Scaled from ASTM D412

Experimental Methods: Monotonic Loading

- Stress state dependence
  - Tension
    - Strain controlled from extension to get local strain rate
    - Strain in the gage measured by laser extensometer
  - Compression
    - Extensometer mounted on platens to remove compliance
    - Strain controlled from extensometer
- Rate dependence
  - Strain rates of 0.001, 0.01, 0.1, 1200, 2000, 2600, 3000 /s
- Temperature dependence
  - -5C, 23C and 50C

Experimental Methods: Fatigue Loading

- Uniaxial tension
- Servo-hydraulic load frame
- R = 0.5, freq = 2 Hz
- Δε/2 = 20.3, 22.3, 28.1, 31.9 and 36.3%
- Displacement control
- Displacement-strain correlation made using laser extensometer

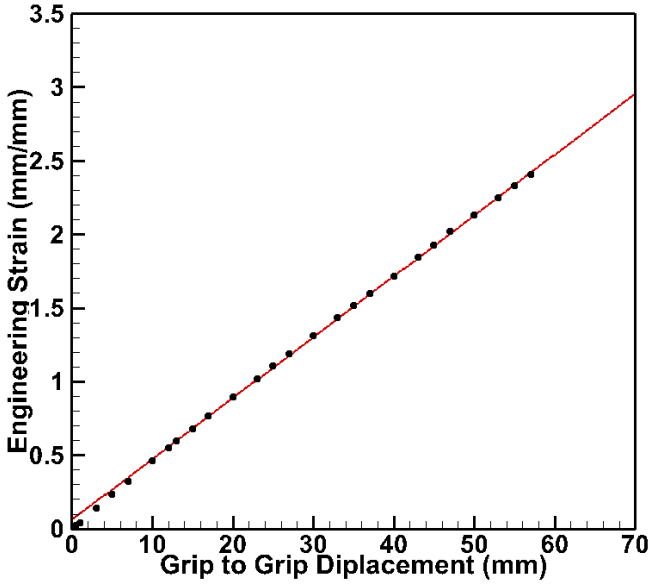

Results: DMA

- Storage modulus curve shows two transition temperatures
  - First corresponds to the glass transition temperature (Tg) at -40° C
  - Second at -10° C possibly due to fillers

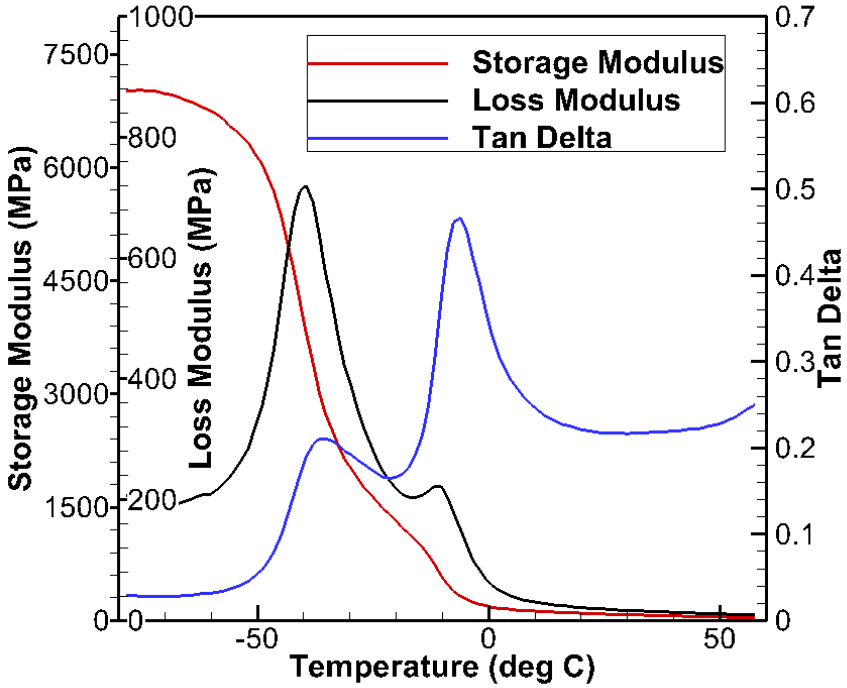

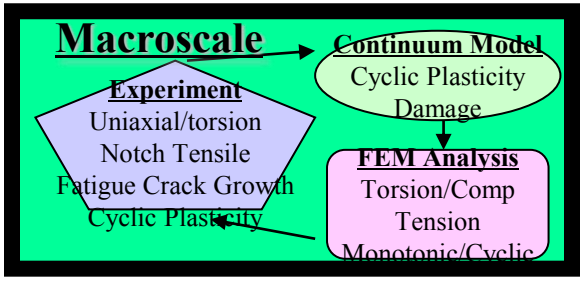

Results: Rate Dependence

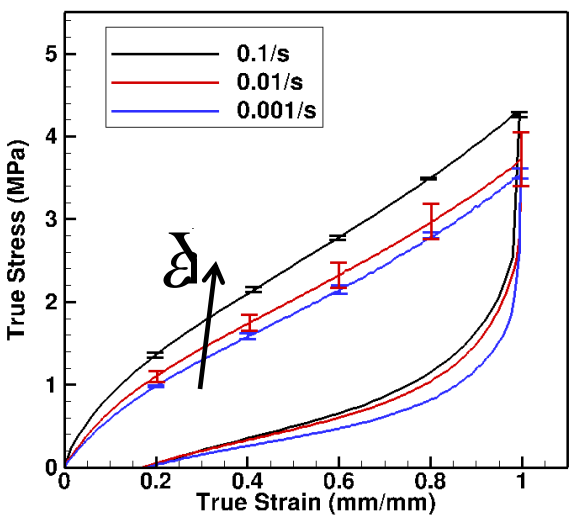

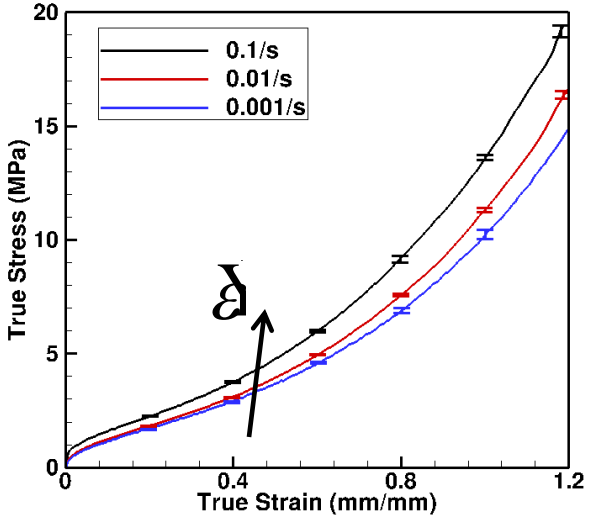

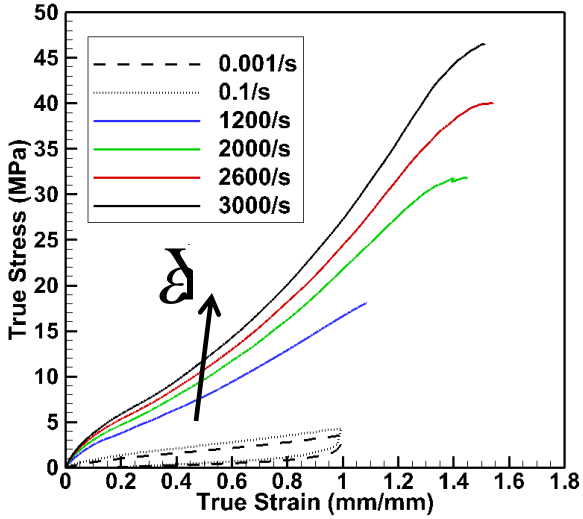

- Rate dependence – material stiffened with increasing strain rate
- Compression – strong hysteresis and residual plastic strain

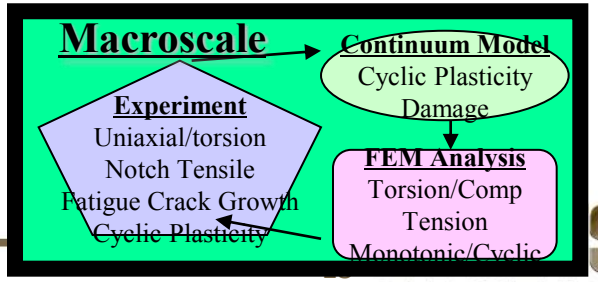

Results: Temperature Dependence

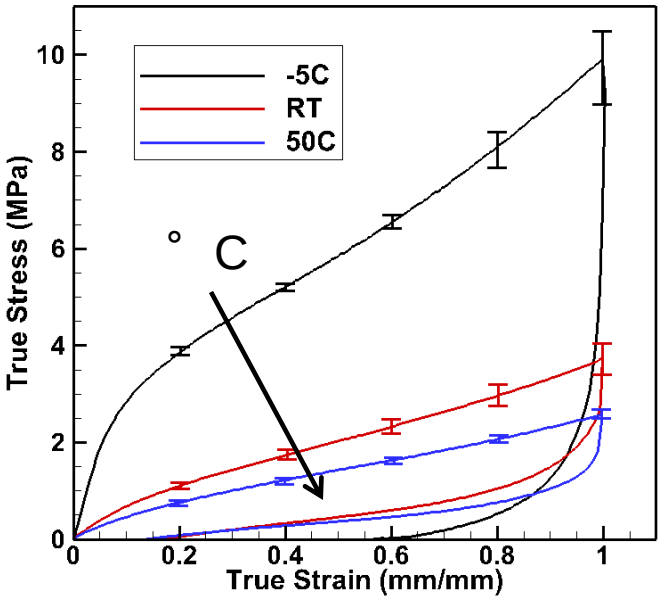

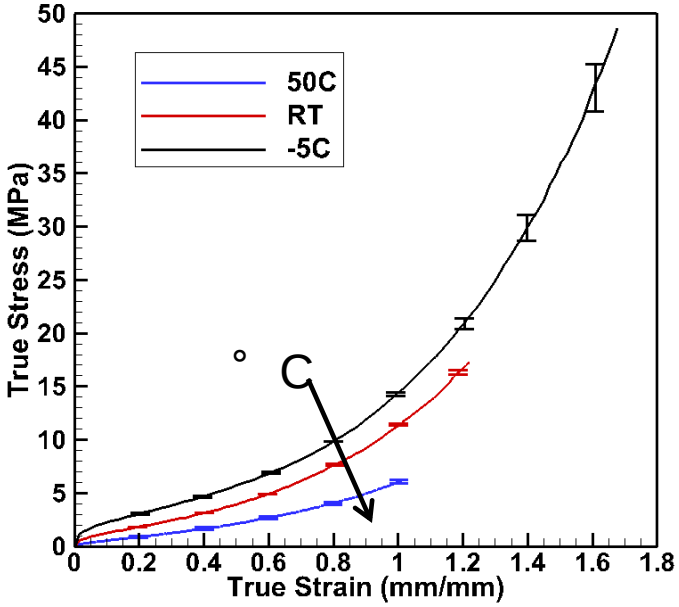

- Temperature dependence – material softened and had an increase in strain to failure at higher temperatures

Results: Microstructure for Monotonic Loading

- Particle debonding
  - Major mechanism of failure
  - 0.5 – 200 μm particles debonded during deformation
  - Large particles are (1) agglomerations of aluminosilicate (clay) and (2) ground calcium carbonate

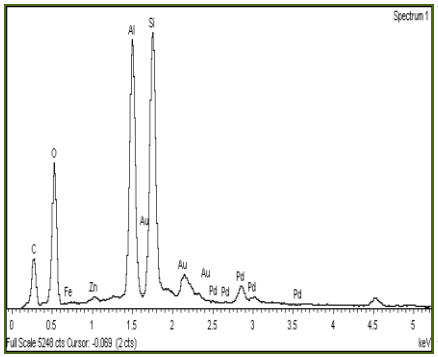

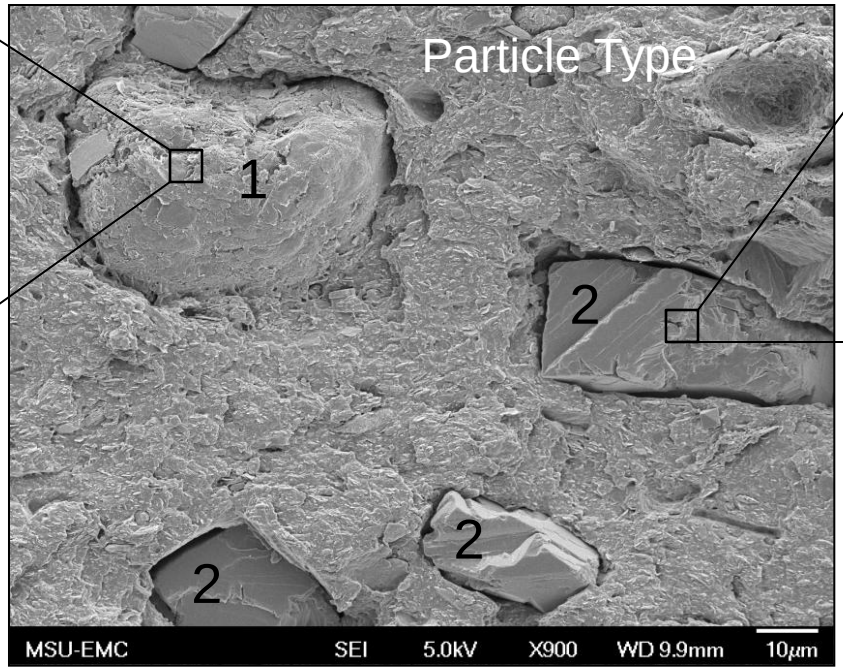

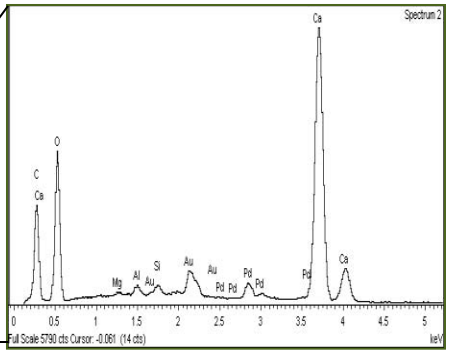

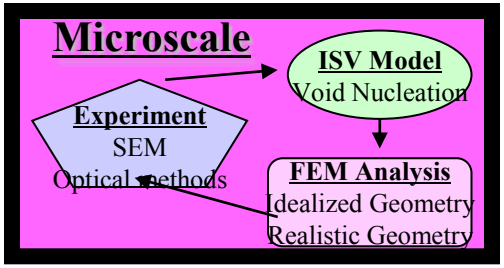

Results: Microstructure for Monotonic Loading - ε̇ = 0.1/s

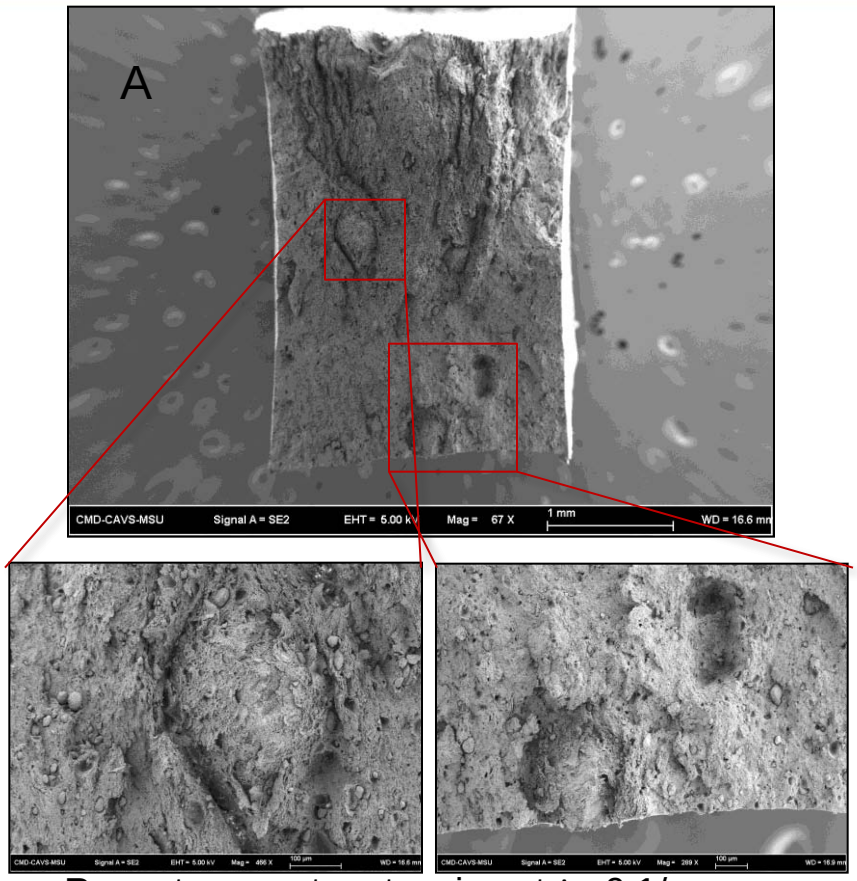

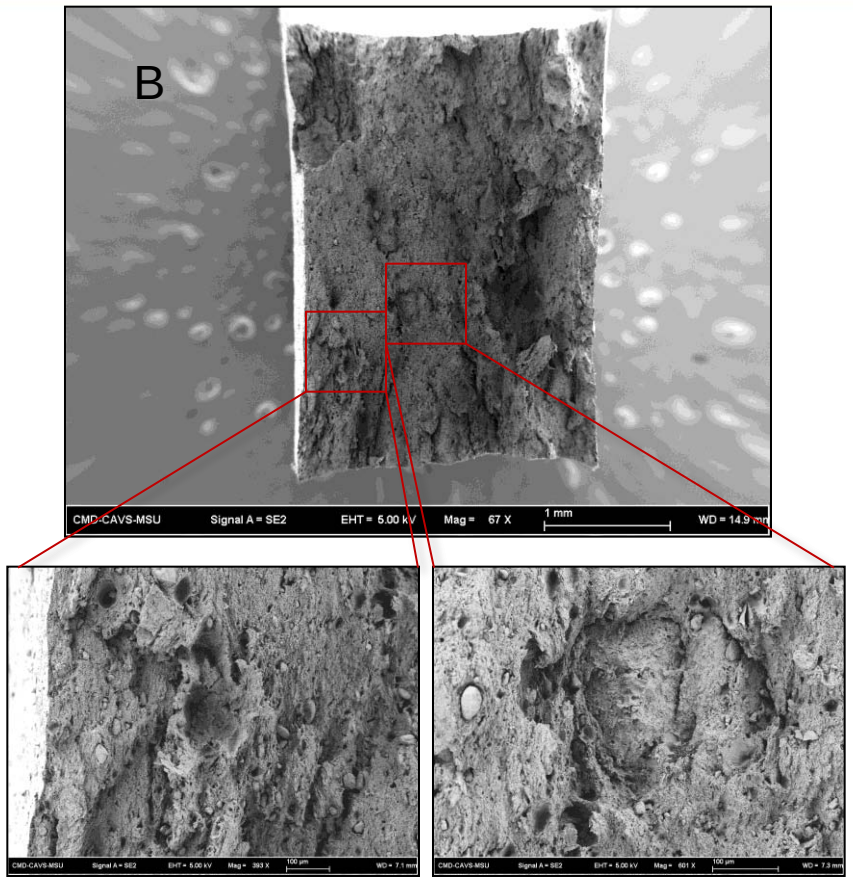

- Room temperature tension at ε̇= 0.1/s
- Specimen A failed at a lower strain than specimen B
- Specimen A showed a slightly weaker stress-strain response than specimen B
- Due to the large agglomerates of undispersed aluminosilicate and particles debonding from the matrix

Results: Microstructure for Monotonic Loading - $\dot{\varepsilon}$ = 0.01/s

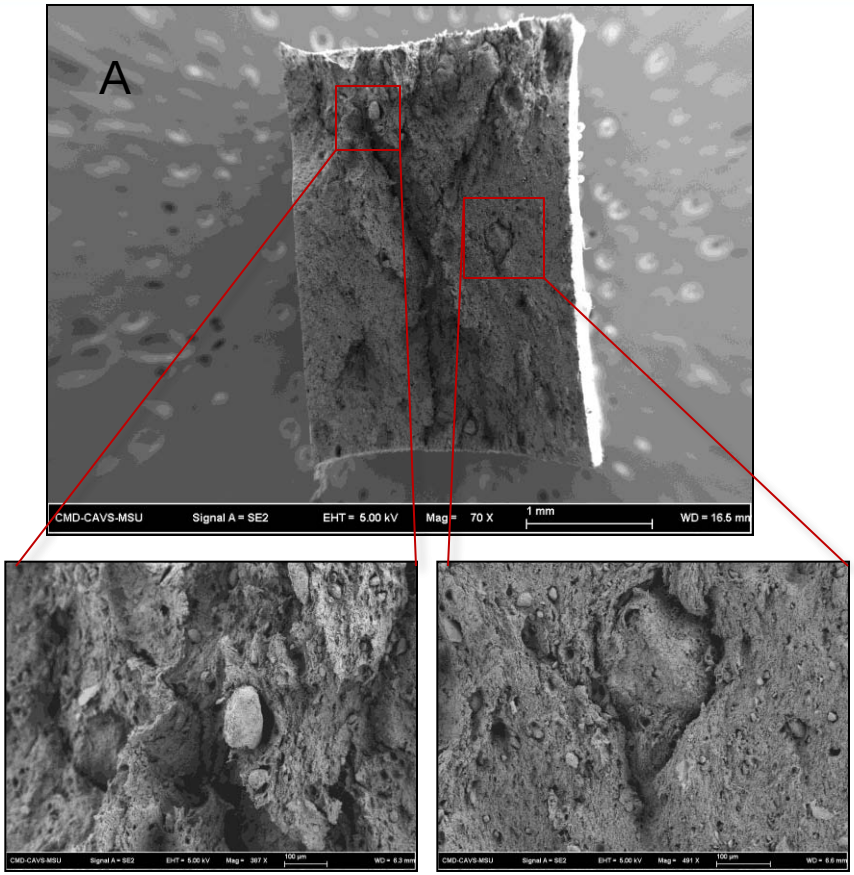

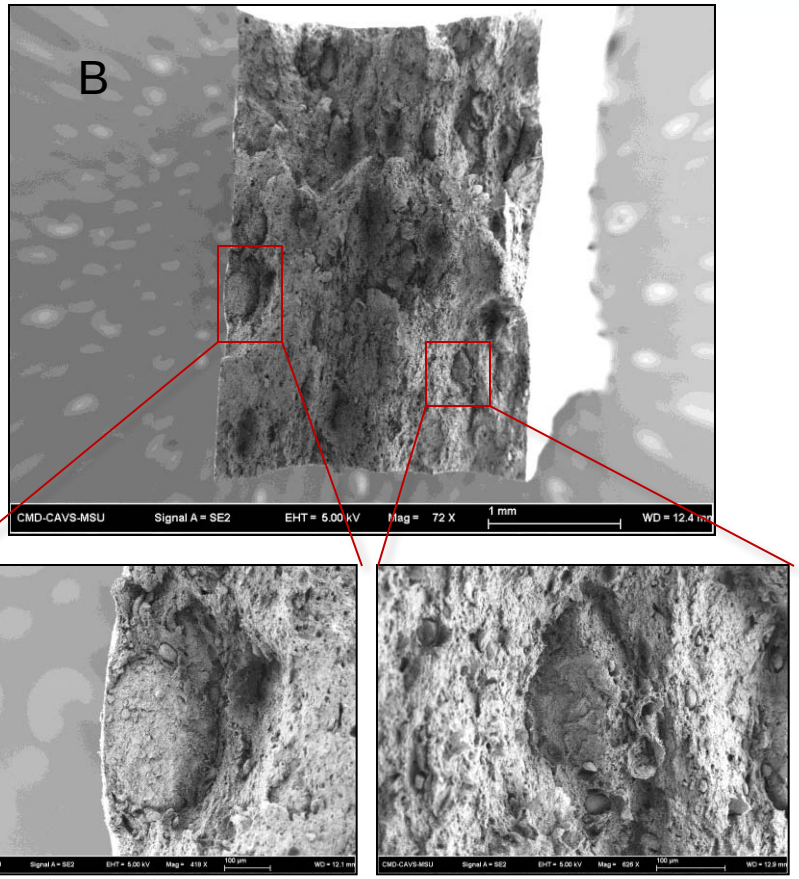

- Room temperature tension at $\dot{\varepsilon}$= 0.01/s
- Specimen A failed at a lower strain than specimen B
- Due to the large agglomerates of undispersed aluminosilicate and particle debonding

Results: Microstructure for Monotonic Loading - ε̇ = 0.001/s

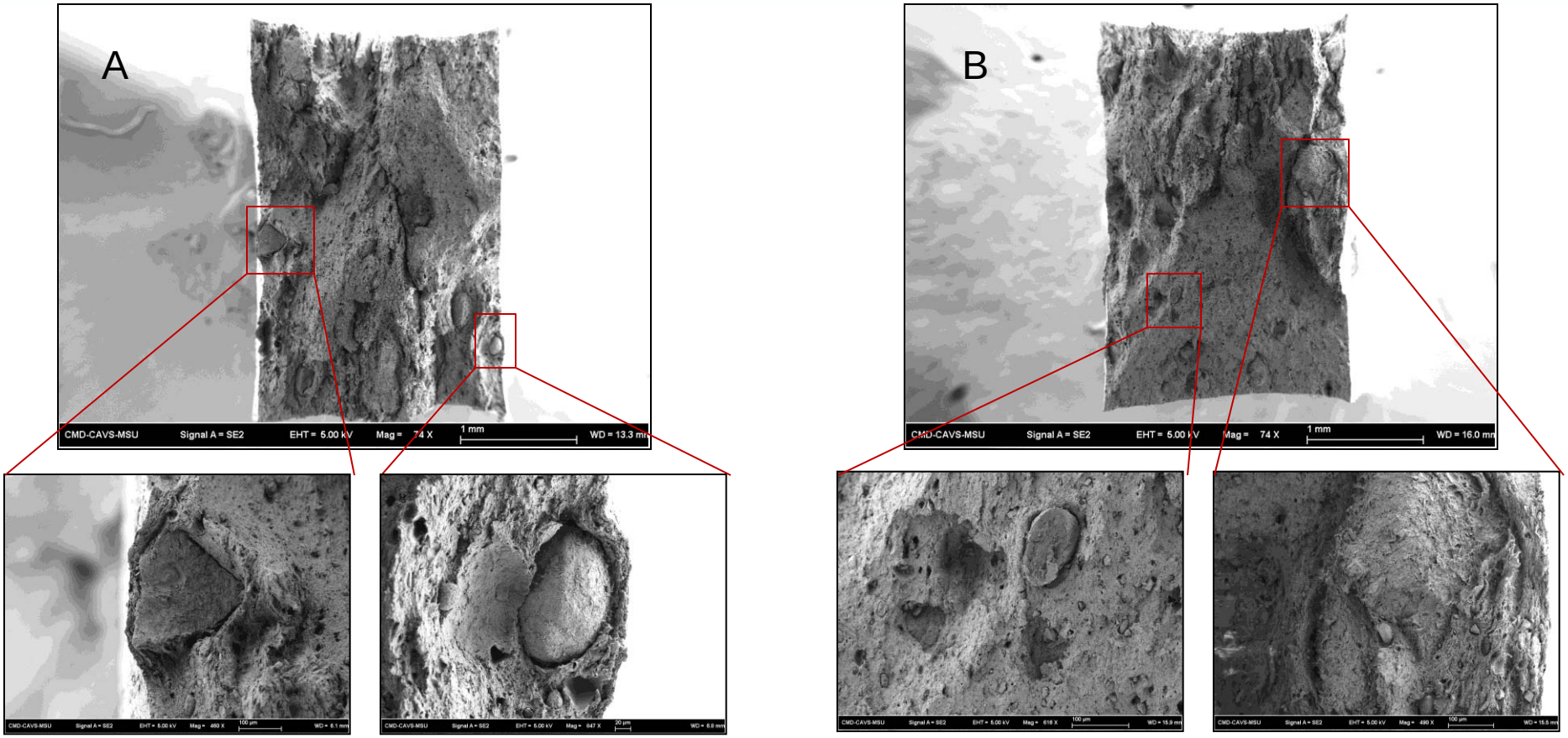

- Room temperature tension at ε̇= 0.001/s
- Specimen A failed at a lower strain than specimen B
- Due to the large agglomerates of undispersed aluminosilicate and particle debonding

Macroscale MSU ISV/MSF Models Implementation and Use

MSTV MODELING AND SIMULATION, TESTING AND VALIDATION

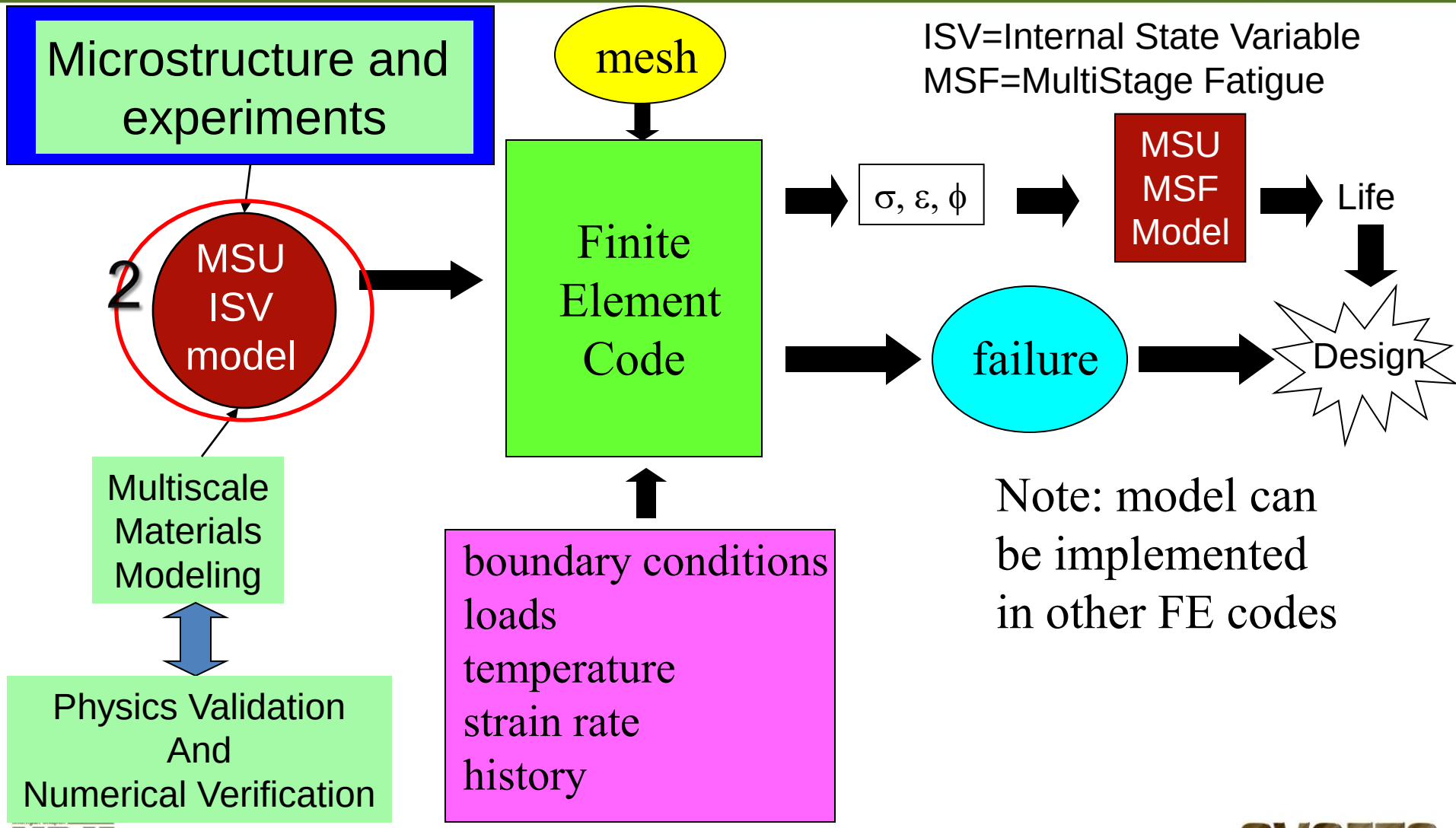

ISV Model: Approach

- Large variety of models exists for polymers: Krempl (1995), Tervoort (1998), Boyce et al. (1988), Richeton et al. (2007), L. Anand et al. (2009),…

Rheological representation of the constitutive model

- **Model generally used for polymers are:**
  - **based on spring/dashpot**

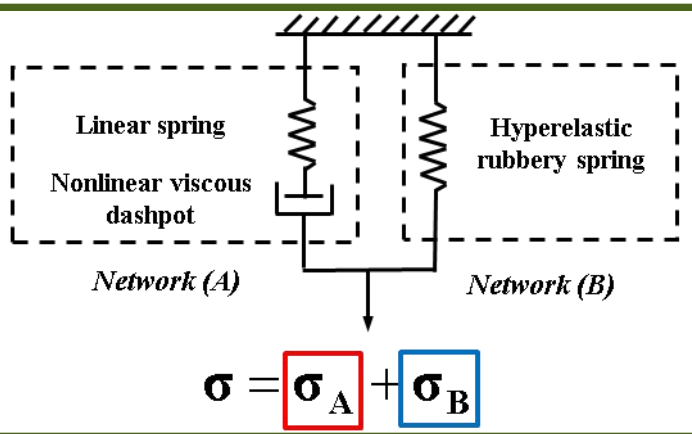

Hierarchical Multiscale Approach

- **Development of ISV material model:**

- Kinematics
- Thermodynamics → select physically-based ISVs

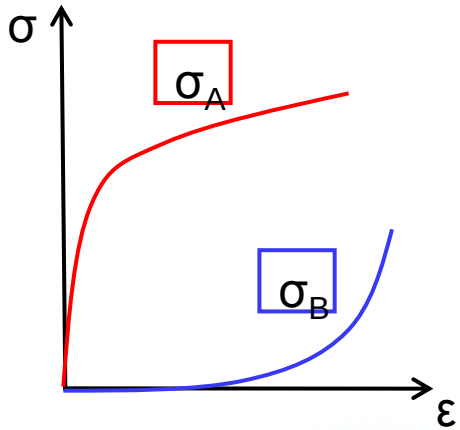

ISV Model: Extension to Elastomers

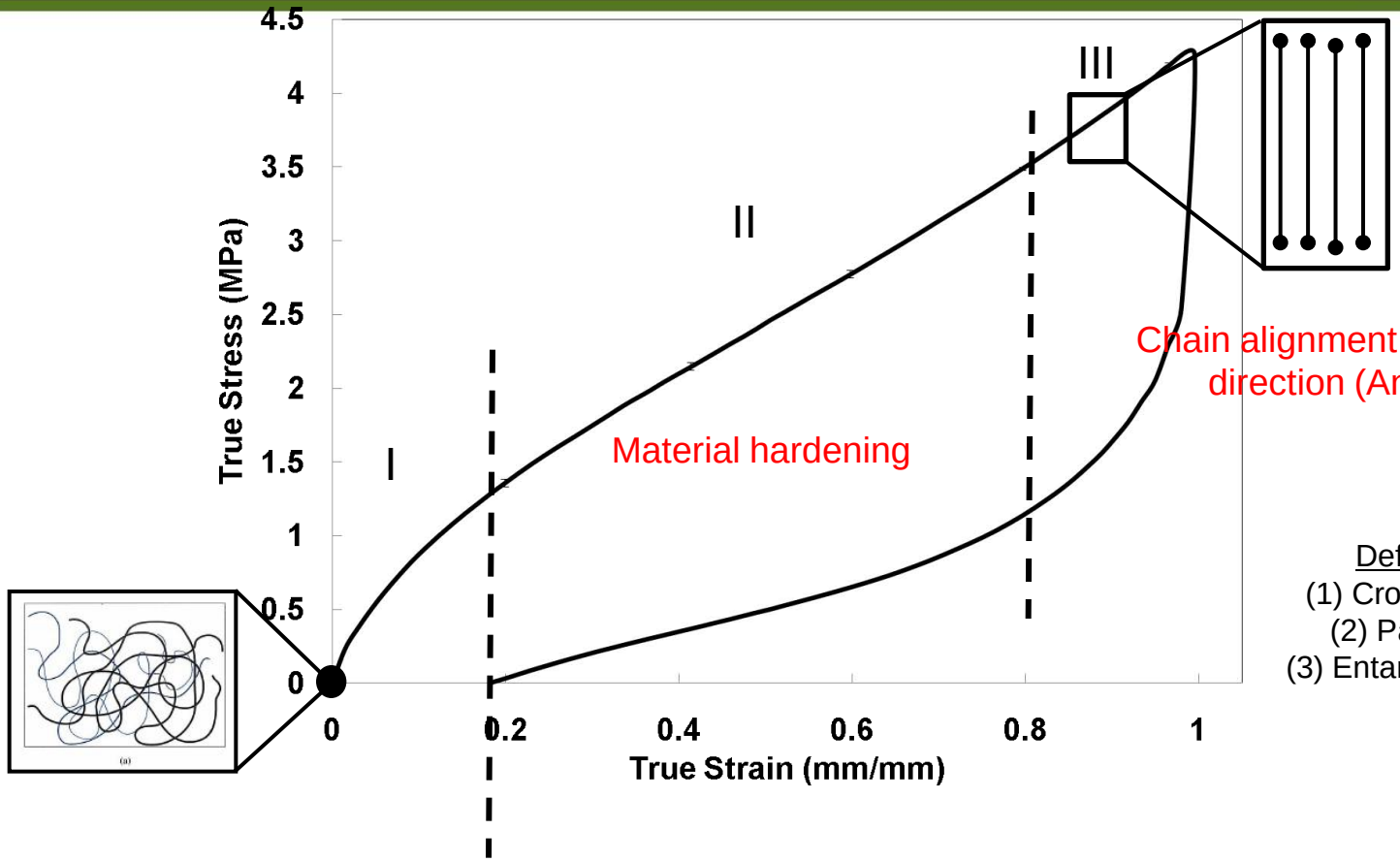

Defects:
(1) Crosslinking
(2) Particles
(3) Entanglements

Regime I: Hyperelastic mechanism induced by bond stretching/rotation

Regime II: Strain hardening induced by crosslinking, entanglements, and particles

Regime III: Chain alignment and chain stretching between crosslinking and possible chain crystallization

ISV Model: Development for Amorphous Polymers

$$\mathbf{F} = \mathbf{F}^{\mathbf{e}}\mathbf{F}^{\mathbf{p}}$$

$\mathbf{F}^{\mathbf{e}}$: elastic mechanisms such as bond stretching and chains rotation/torsion inducing the different conformations of the intramolecular structure

$\mathbf{F}^{\mathbf{p}}$: time-dependent inelastic mechanisms such as permanent chains stretching and rotating but also the dissipative mechanism due to the relative slippage of molecular chains

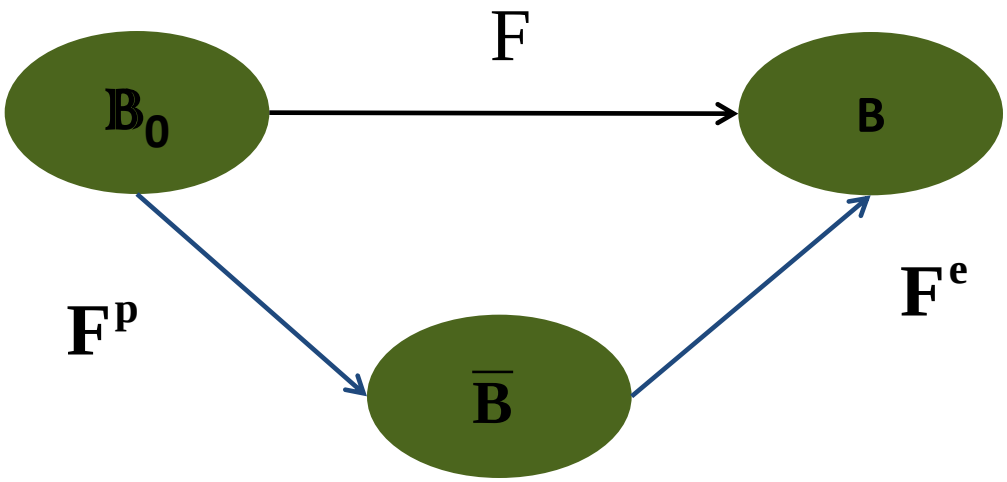

ISV Model: Kinematics and Thermodynamics

- Multiplicative decomposition of deformation gradient

$\mathbf{F} = \mathbf{F^e F^p}$ Deformation gradient

Kroner-Lee decomposition

$J^e = \det \mathbf{F^e}\ ;\ J^p = \det \mathbf{F^p}\ ;$

- Kinematics $\rightarrow$ velocity gradient $\mathbf{l}$:

$\mathbf{l} = \dot{\mathbf{F}}\mathbf{F}^{-1}$

$\mathbf{l} = \mathbf{l^e} + \mathbf{F^e}\bar{\mathbf{L}}^{\mathbf{p}}\mathbf{F^{e-1}}$

  - $\mathbf{l^e} = \dot{\mathbf{F}}^{\mathbf{e}}\mathbf{F^{e-1}}\ ;\quad \mathbf{l^e} = \mathbf{d^e} + \mathbf{w^e}$
  - $\bar{\mathbf{L}}^{\mathbf{p}} = \dot{\mathbf{F}}^{\mathbf{p}}\mathbf{F^{p-1}}\quad \bar{\mathbf{L}}^{\mathbf{p}} = \bar{\mathbf{D}}^{\mathbf{p}} + \bar{\mathbf{W}}^{\mathbf{p}}$

Decomposition into symmetric and skew part

- Assumption on plastic flow
  - $J^p = 1$ Flow is incompressible
  - $\bar{\mathbf{W}}^{\mathbf{p}} = \mathbf{0}$ Flow is irrotational
- Thermodynamics

Clausius-Duhem inequality (Gurtin and Coleman, 1967; Gurtin and Anand, 2003)

$$\frac{D}{Dt}\int_B J^{e-1}\dot{\psi}\,dv \le \int_B \boldsymbol{\sigma} : \mathbf{l}\,dv$$

localize integrals

$$\bar{\mathbf{S}} : \mathbf{F}^{eT}\mathbf{d}^{\mathbf{e}}\mathbf{F}^{\mathbf{e}} + \bar{\mathbf{M}} : \bar{\mathbf{D}}^{\mathbf{p}} - \dot{\bar{\psi}} \ge 0$$

$\bar{\mathbf{S}} = \mathbf{J}^{e-1}\mathbf{F}^{e-1}\boldsymbol{\sigma}\mathbf{F}^{e-T}$

$\bar{\mathbf{M}} = \bar{\mathbf{C}}^{e}\bar{\mathbf{S}}$

ISV Model: Kinematics and Thermodynamics

- Helmholtz Free Energy:

strain/stretch -like internal state variables

$$\overline{\psi} = \hat{\overline{\psi}}\left(\overline{\mathbf{C}}^{\mathbf{e}}, \overline{\Pi}\right); \; \overline{\Pi} = \left\{\overline{\xi}_1, \overline{\xi}_2, \overline{\mathbf{E}}^{\overline{\beta}}\right\}$$

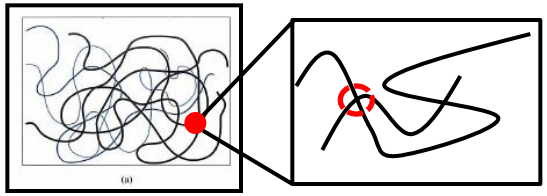

$\overline{\xi}_1$: Strain field induced by internal strain field related to the intermolecular chain interaction in Regime I and II (van der Waals forces mainly)

$\overline{\xi}_2$: Strain field induced internal strain field related to the crystallization in Regime III

$\overline{\mathbf{E}}^{\overline{\beta}}$: Stretch-like tensor giving direction-dependent (kinematic) hardening effect induced by the chain stretching between entanglements/crosslinking at large strain

$$\rightarrow \quad \dot{\overline{\psi}} = \frac{\partial \hat{\overline{\psi}}}{\partial \overline{\mathbf{C}}^{\mathbf{e}}} : \dot{\overline{\mathbf{C}}}^{\mathbf{e}} + \frac{\partial \hat{\overline{\psi}}}{\partial \overline{\xi}_1} : \dot{\overline{\xi}}_1 + \frac{\partial \hat{\overline{\psi}}}{\partial \overline{\xi}_2} : \dot{\overline{\xi}}_2 + \frac{\partial \hat{\overline{\psi}}}{\partial \overline{\boldsymbol{\beta}}} : \dot{\overline{\boldsymbol{\beta}}}$$

- Clausius-Duhem Inequality:

$$\left[\overline{\mathbf{S}} - 2\frac{\partial \overline{\psi}}{\partial \overline{\mathbf{C}}^{\mathbf{e}}}\right] : \mathbf{F}^{\mathbf{e}\mathbf{T}}\mathbf{d}^{\mathbf{e}}\mathbf{F}^{\mathbf{e}} + \overline{\mathbf{M}} : \overline{\mathbf{D}}^{\mathbf{p}} - \left(\underbrace{\frac{\partial \hat{\overline{\psi}}}{\partial \overline{\xi}_1}}_{\overline{\kappa}_1} : \dot{\overline{\xi}}_1 + \underbrace{\frac{\partial \hat{\overline{\psi}}}{\partial \overline{\xi}_2}}_{\overline{\kappa}_2} : \dot{\overline{\xi}}_2 + \underbrace{\frac{\partial \hat{\overline{\psi}}}{\partial \overline{\boldsymbol{\beta}}}}_{\overline{\boldsymbol{\alpha}}} : \dot{\overline{\boldsymbol{\beta}}} \right) \geq 0$$

ISV Model: Summary

Elasticity: Cauchy Stress

$$\mathbf{F} = \mathbf{F}^{e}\mathbf{F}^{p};\ \mathbf{F}^{e} = \mathbf{R}^{e}\mathbf{U}^{e};\ \mathbf{F}^{e*} = \left(J^{e}\right)^{-1/3}\mathbf{F}^{e};\ \mathbf{b}^{e*} = \mathbf{F}^{e*}\mathbf{F}^{e*T}$$

$$\boldsymbol{\tau} = \mathbf{F}^{e}\bar{\mathbf{S}}\mathbf{F}^{eT};\quad \boldsymbol{\tau} = \hat{\mu}_{B}^{*}\,\mathbf{dev}\left(\mathbf{b}^{e*}\right) + \hat{K}_{B}\left(J^{e}\right)\mathbf{1};\quad \boldsymbol{\sigma} = J^{e-1}\,\boldsymbol{\tau}$$

Inelastic Flow rule

$$\dot{\mathbf{F}}^{p} = \bar{\mathbf{L}}^{p}\mathbf{F}^{p};\ \bar{\mathbf{L}}^{p} = \bar{\mathbf{D}}^{p} + \bar{\mathbf{W}}^{p};\ \bar{\mathbf{D}}^{p} = \frac{1}{\sqrt{2}}\dot{\gamma}^{p}\,\bar{\mathbf{N}}^{p};\ \bar{\mathbf{W}}^{p} = 0$$

$$\dot{\gamma}^{p} = \dot{\gamma}_{0}^{p}\left[\sinh\left(\frac{\bar{\tau} - \left(\bar{\kappa}_{1} + \alpha_{p}\bar{\pi}\right)}{Y}\right)\right]^{m};\ \bar{\mathbf{N}}^{p} = \frac{\overline{\mathbf{DEV}}\left(\bar{\mathbf{M}} - \bar{\boldsymbol{\alpha}}\right)}{\left\|\overline{\mathbf{DEV}}\left(\bar{\mathbf{M}} - \bar{\boldsymbol{\alpha}}\right)\right\|}$$

$$\bar{\tau} = \frac{1}{\sqrt{2}}\left\|\overline{\mathbf{DEV}}\left(\bar{\mathbf{M}} - \bar{\boldsymbol{\alpha}}\right)\right\|\ ;\ \bar{\pi} = -\frac{1}{3}\overline{\mathrm{Tr}}\left(\bar{\mathbf{M}}\right)$$

$$\bar{\kappa}_{1} = C_{\kappa_{1}}\,\bar{\xi}_{1};\quad \bar{\boldsymbol{\alpha}} = C_{\alpha}\,\bar{\mathbf{E}}^{\bar{\beta}}$$

Evolution Equations

$$\dot{\bar{\xi}}_{1}^{*} = h_{0}\left(1 - \frac{\bar{\xi}_{1}}{\bar{\xi}^{*}}\right)\dot{\gamma}^{p};$$

$$\dot{\bar{\mathbf{E}}}^{\bar{\beta}} = \left(R_{s_1} + R_{s_2}\left\|\bar{\mathbf{E}}^{\bar{\beta}}\right\|^{2}\right)\bar{\mathbf{D}}^{p}$$

Parameters $\left\{\mu, \dot{\gamma}_{p}^{0}, m, \alpha_{p}, Y, h_{0}, \bar{\xi}_{10}, \bar{\xi}_{0}^{*}, \bar{\xi}_{sat}^{*}, R_{S1}, R_{S2}, C_{\kappa_1}, C_{\alpha}, \lambda_{L}, \mu_{R}\right\}$

ISV Model: Model to Experiment Comparsion

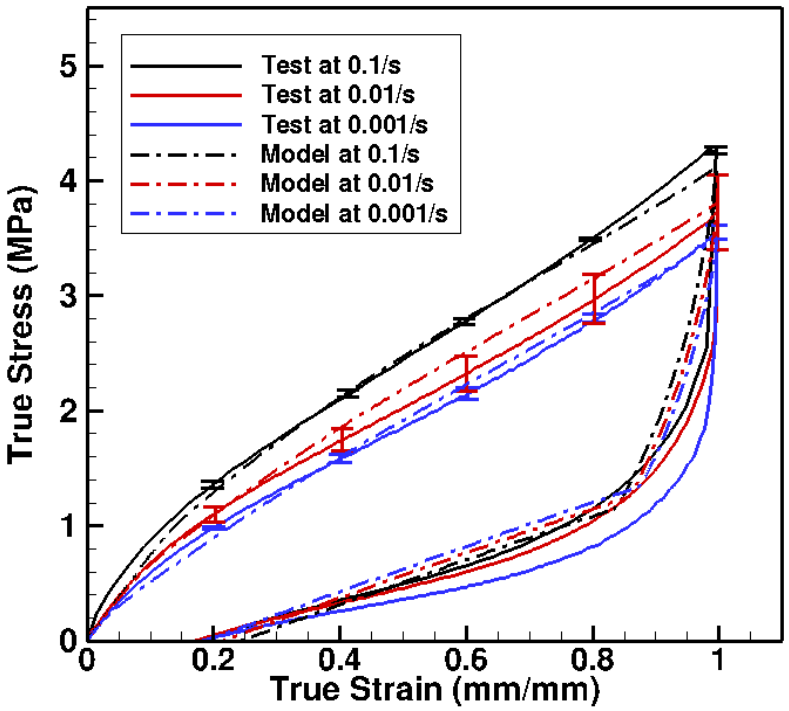

ISV model predicts loading path, unloading path and time dependence

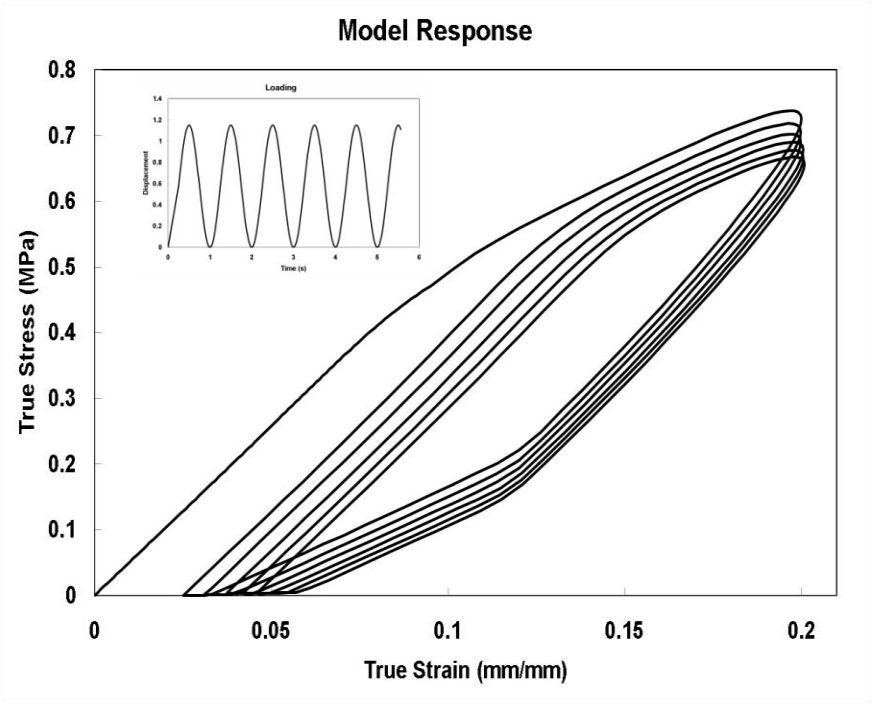

ISV model response under cyclic loading at 1 Hz. It shows significant hysteresis in the first cycle and cyclic relaxation

Macroscale MSU ISV/MSF Models Implementation and Use

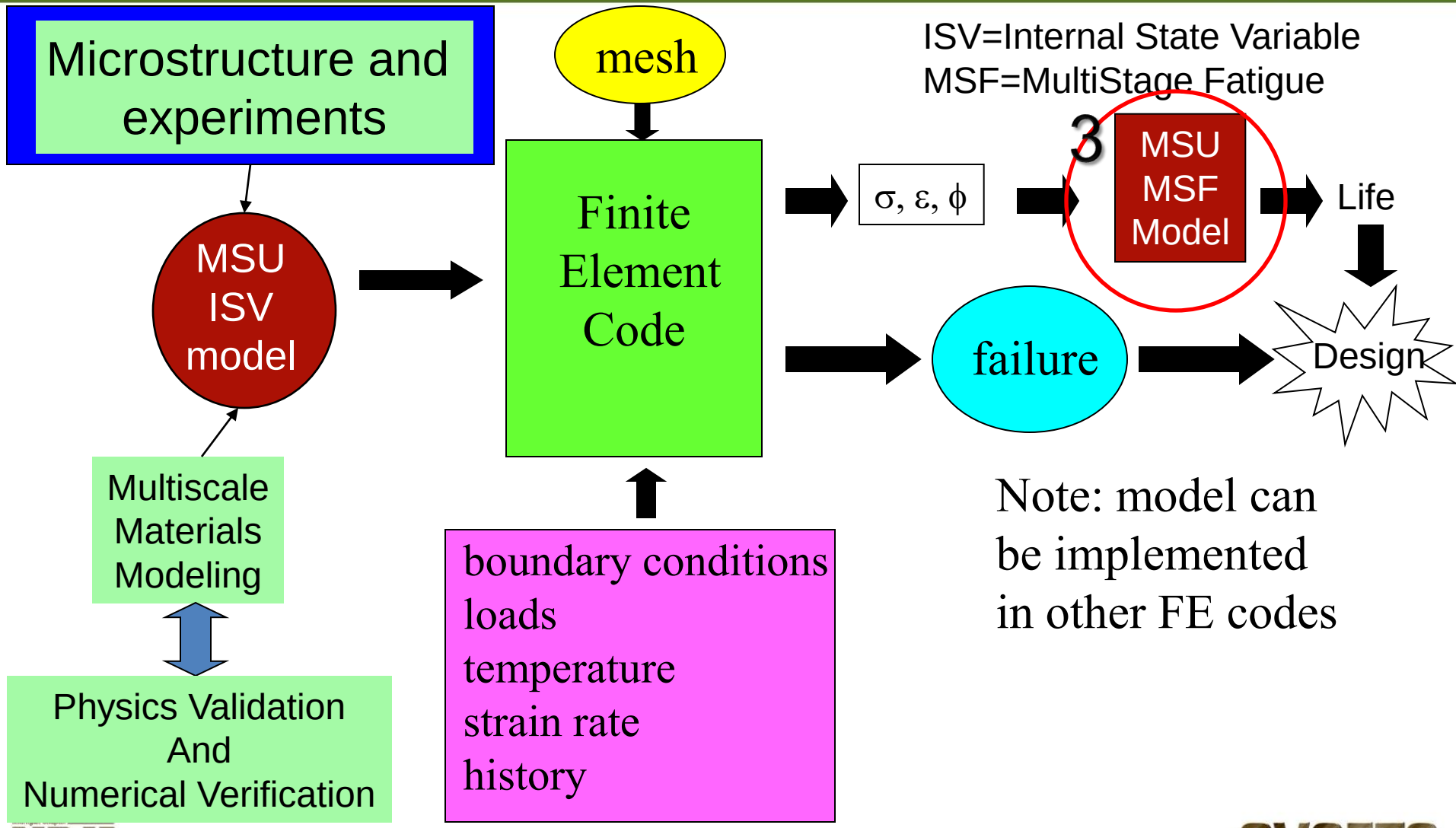

Results: Fatigue Life

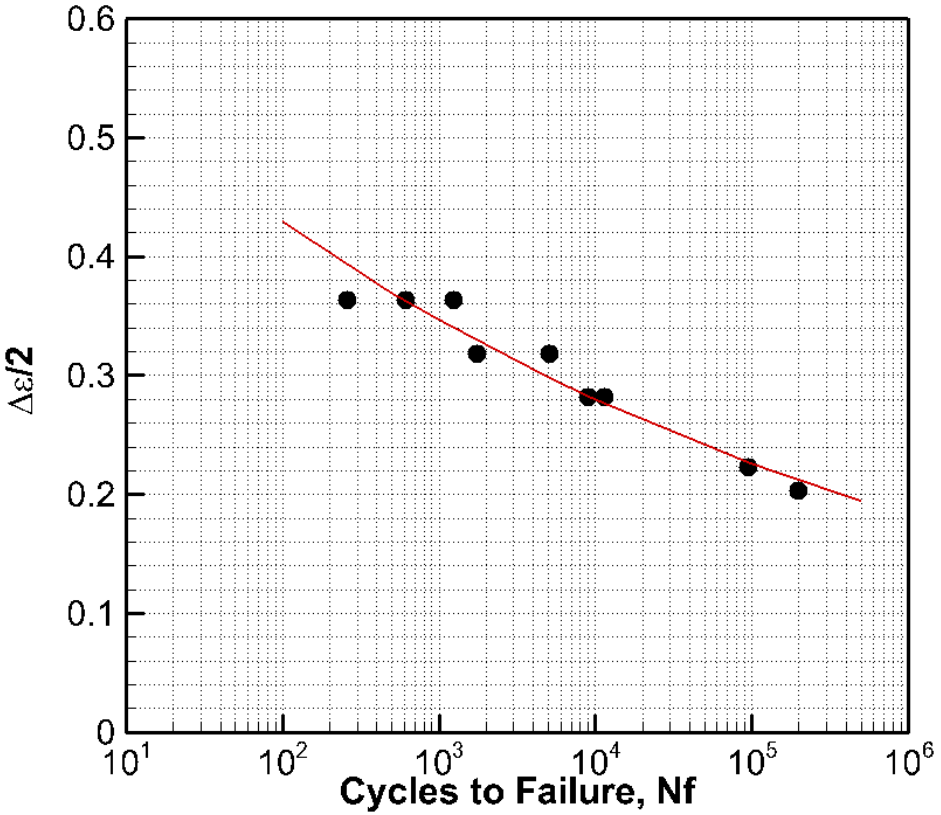

- Power law fit: $\frac{\Delta\varepsilon}{2} = 0.6587\left(N_f\right)^{-0.093}$

Results: Fatigue Loading

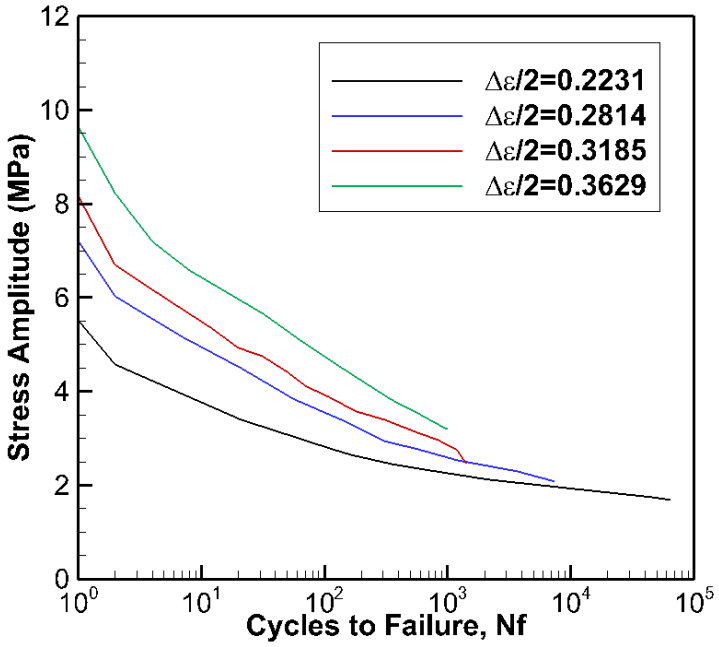

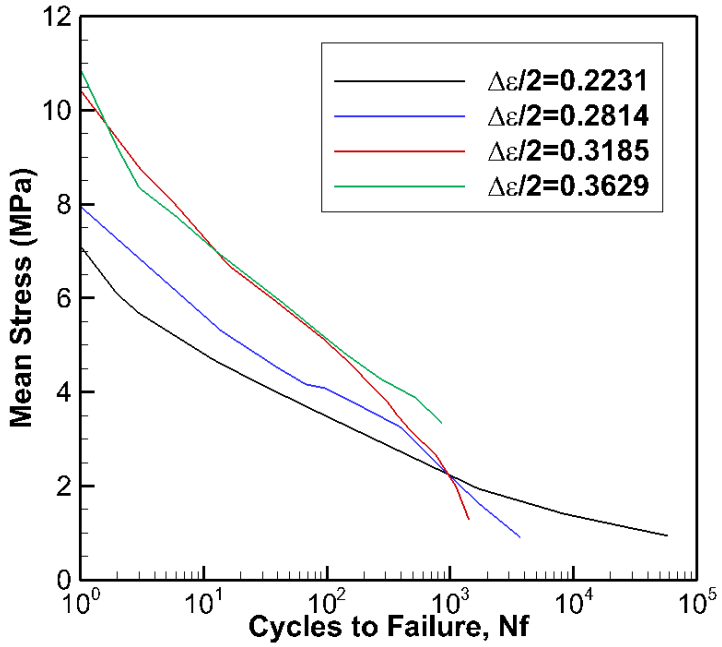

- Significant cyclic stress softening occurred for all strain amplitudes

Results: Hysteresis

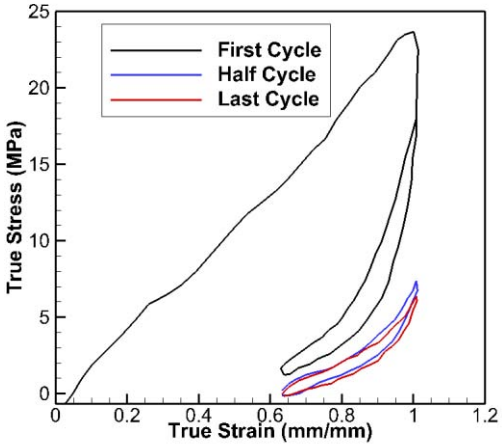

$\Delta\varepsilon/2 = 0.36$

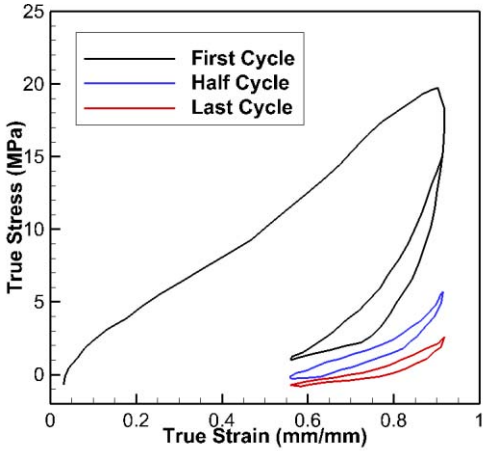

$\Delta\varepsilon/2 = 0.32$

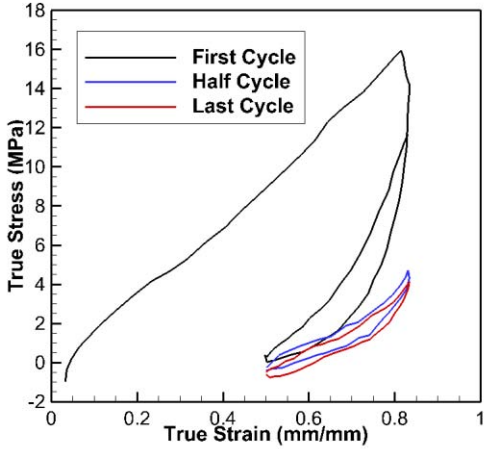

$\Delta\varepsilon/2 = 0.28$

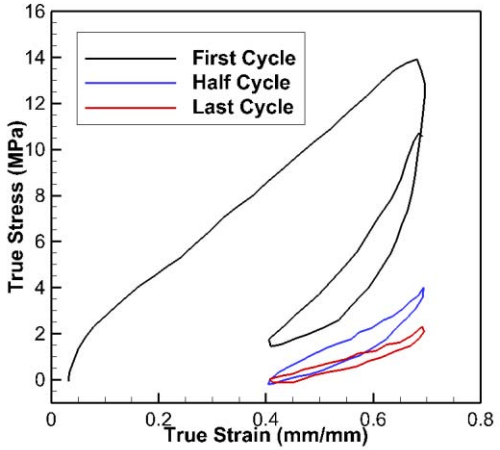

$\Delta\varepsilon/2 = 0.22$

Results: Hysteresis

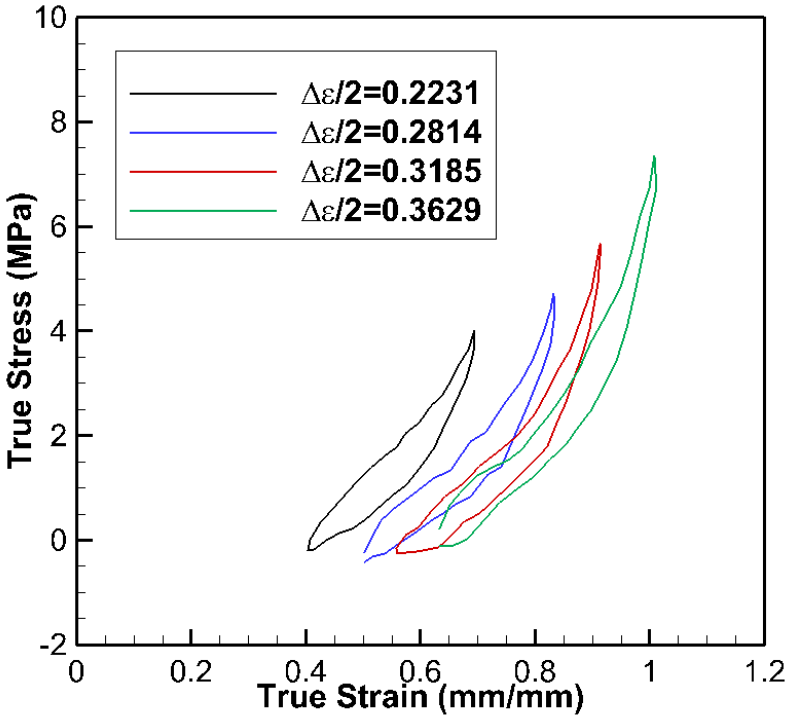

Half cycle at strain amplitudes of 0.22, 0.28, 0.32 and 0.36.

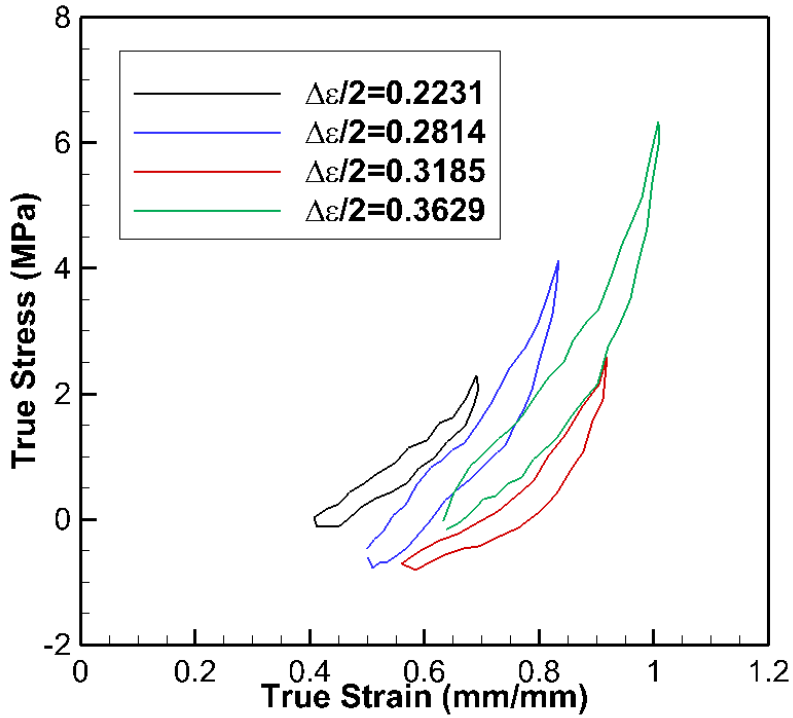

Last cycle at strain amplitudes of 0.22, 0.28, 0.32 and 0.36.

Results: Microstructure for Fatigue Loading

- Particle debonding
  - 0.5 – 200 μm particles debonded during deformation
  - 100 – 200 μm particles initiated significant fatigue cracks
  - 2 particles in length scale of focus: calcium carbonate and agglomerations of aluminosilicate (clay)

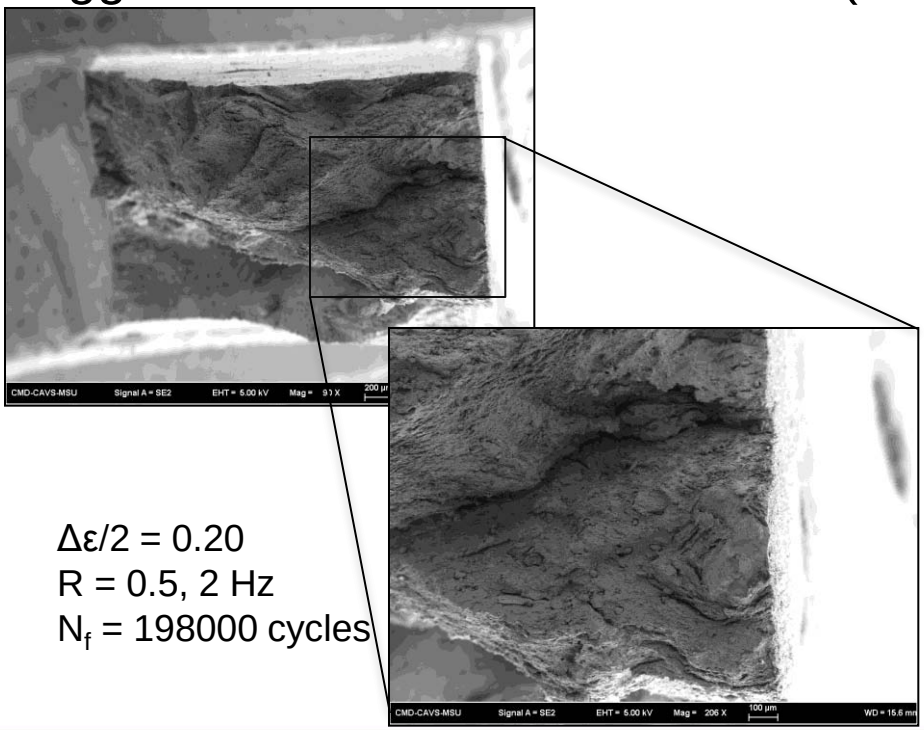

Δε/2 = 0.20
R = 0.5, 2 Hz
N_f = 198000 cycles

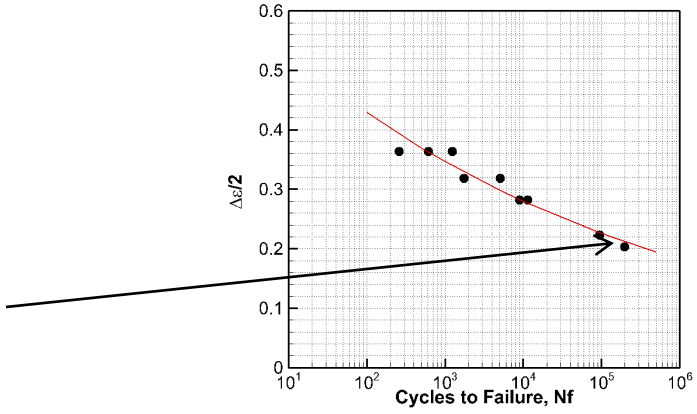

Results: Microstructure for Fatigue Loading

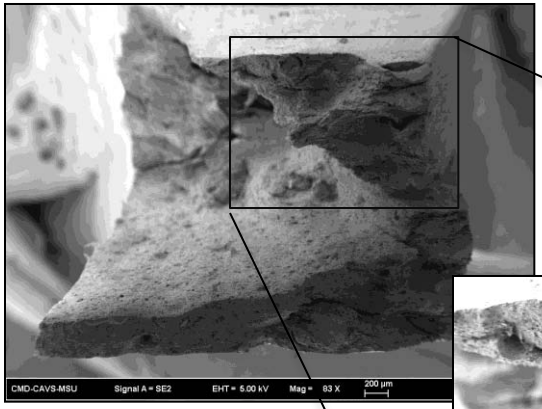

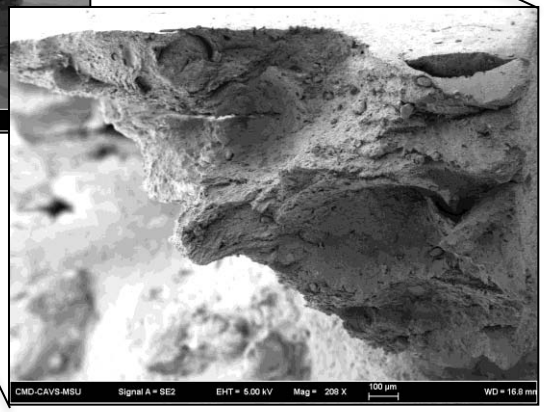

$\Delta\varepsilon/2 = 0.28$
R = 0.5, 2 Hz
N_f = 8908 cycles

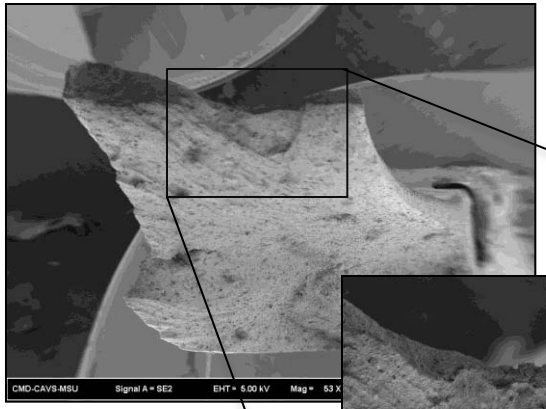

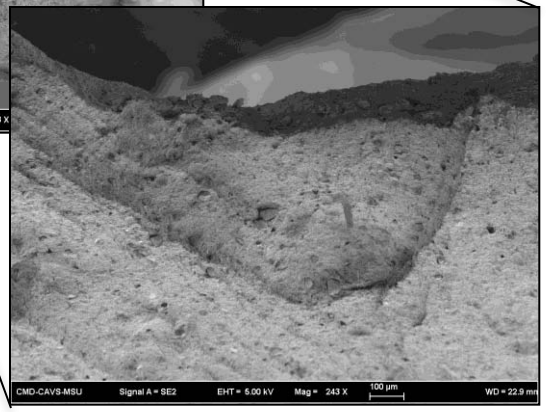

$\Delta\varepsilon/2 = 0.28$
R = 0.5, 2 Hz
N_f = 11439 cycles

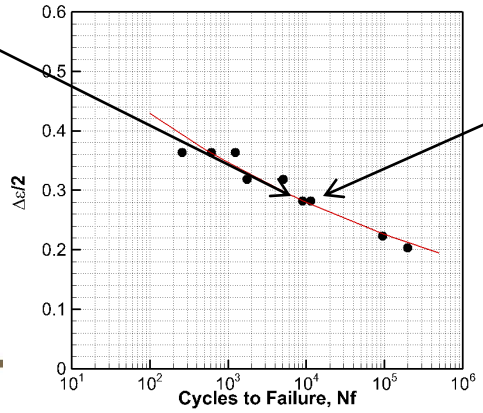

Results: Microstructure for Fatigue Loading

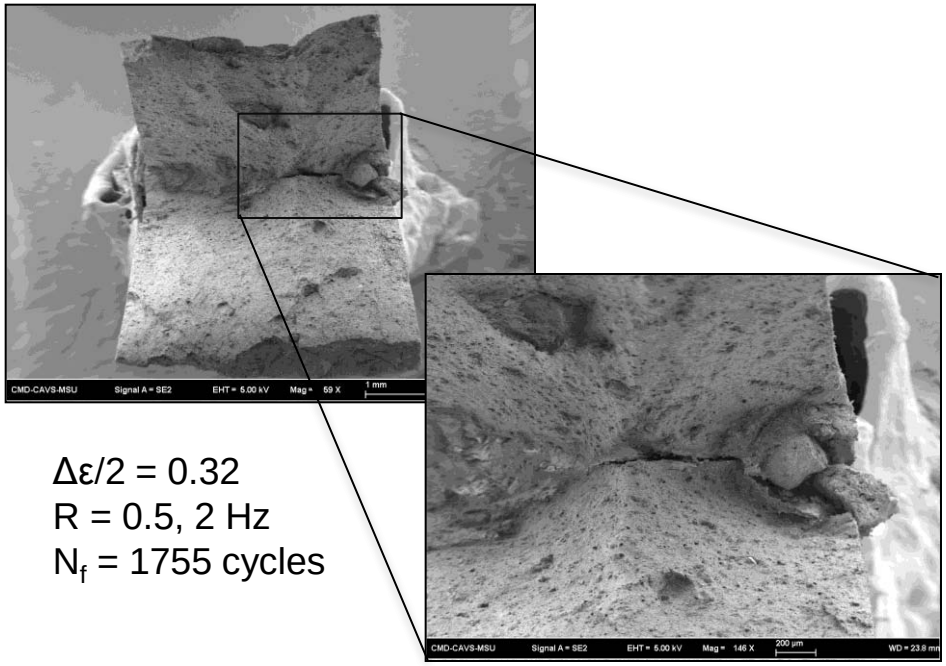

$\Delta\varepsilon/2 = 0.32$
R = 0.5, 2 Hz
N_f = 1755 cycles

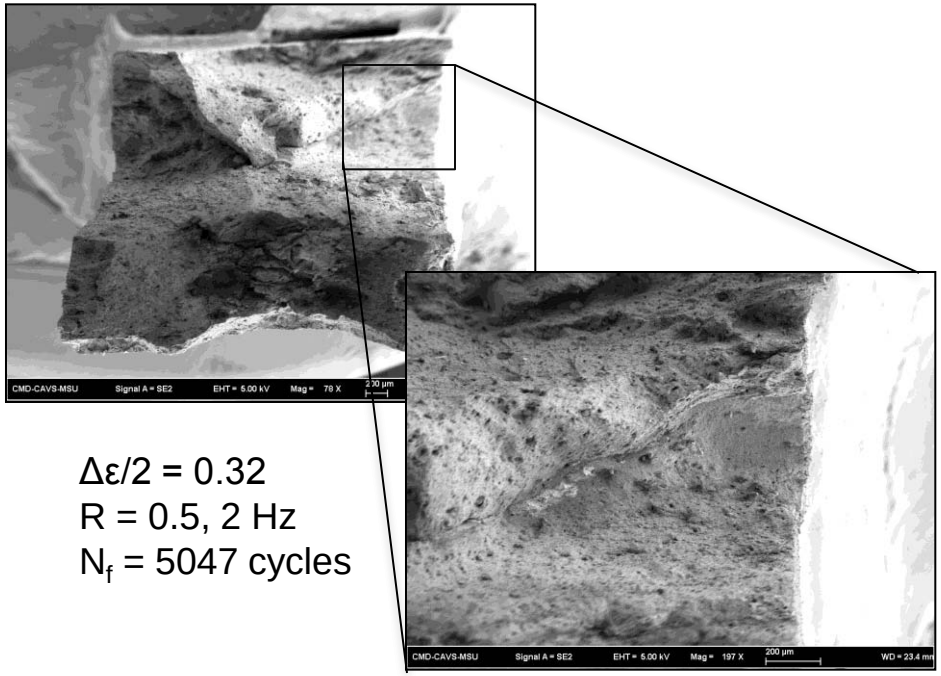

$\Delta\varepsilon/2 = 0.32$
R = 0.5, 2 Hz
N_f = 5047 cycles

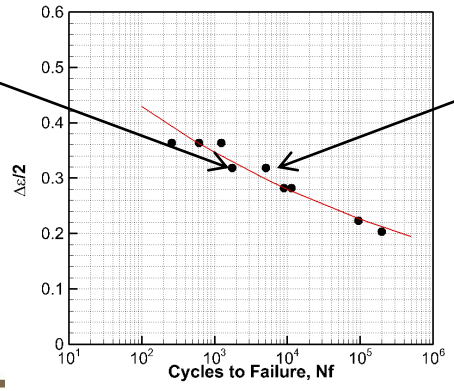

Results: Microstructure for Fatigue Loading

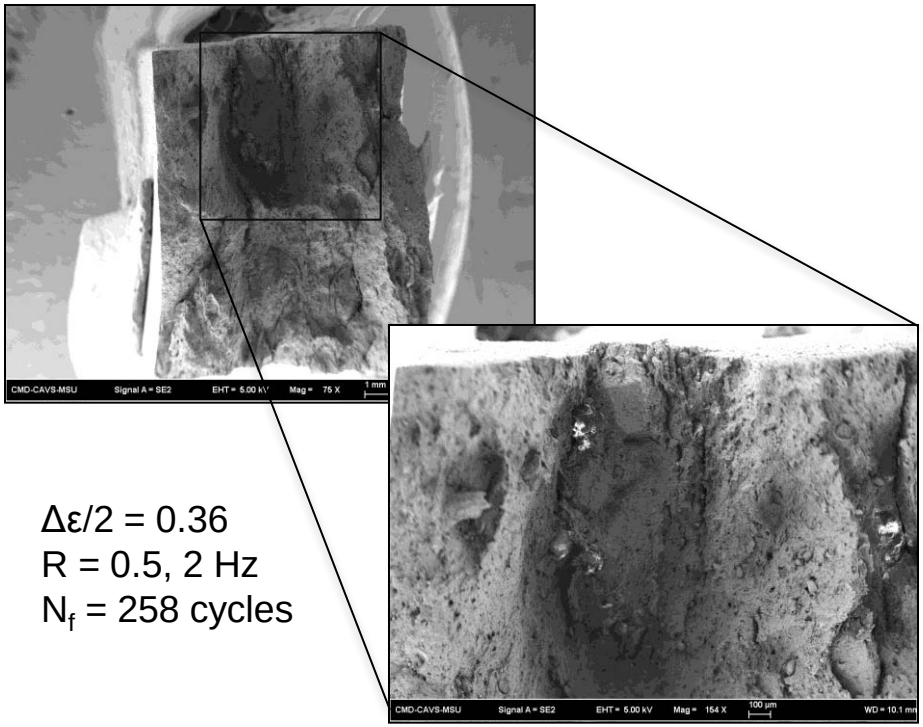

$\Delta\varepsilon/2 = 0.36$
$R = 0.5$, 2 Hz
$N_f = 258$ cycles

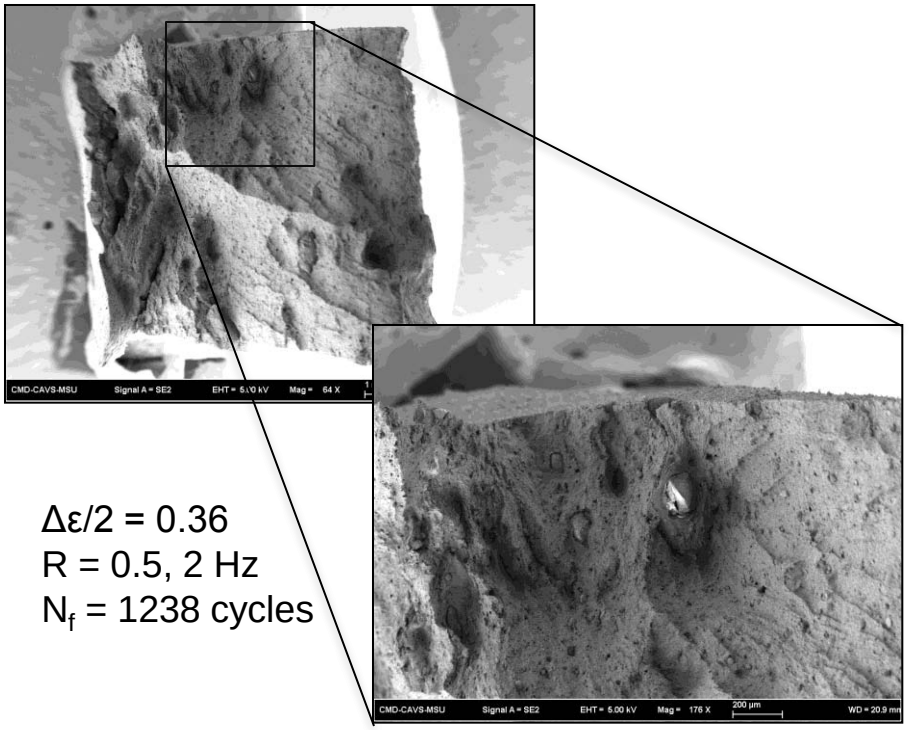

$\Delta\varepsilon/2 = 0.36$
$R = 0.5$, 2 Hz
$N_f = 1238$ cycles

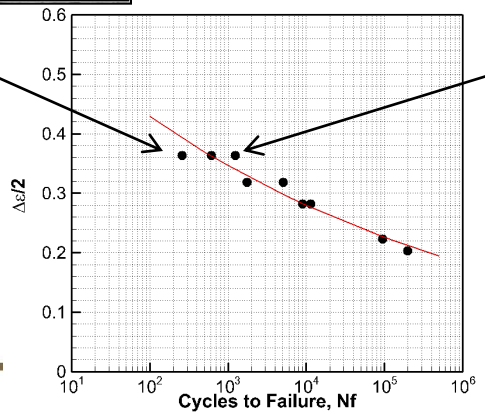

MultiStage Fatigue Model

$$N_{total}=N_{inc}+N_{MSC}+N_{PSC}+N_{LC}$$

Incubation

$$\frac{\Delta\gamma^{P}_{\max}}{2}=C_{inc}N_{inc}^{\alpha} \qquad C_{inc}=C_n+z(C_m-C_n) \text{ and } C_n=0.24\left(1-\langle R\rangle\right)$$

MSC/PSC Growth

$$\left(\frac{da}{dN}\right)_{MSC/PSC}=G\left(\Delta CTD-\Delta CTD_{TH}\right)$$

Initial crack size

$$a_i=0.5625\hat{D}_p$$

$$\Delta CTD=\underbrace{f(\phi)C_{II}(1)\left[\frac{U\Delta\hat{\sigma}}{S_u}\right]^n a}_{\text{HCF loading dominated}}+\underbrace{C_I(1)\left(\frac{\Delta\gamma^{p}_{\max}}{2}\right)^2_{macro}}_{\text{LCF loading dominated}}$$

$$f(\phi)=1+\omega\left\{1-\exp\left(-\frac{\phi}{2\phi_{th}}\right)\right\}$$ Porosity term

ΔCTD_{th} =nonpropagating crack threshold

$$\Delta\hat{\sigma}=2\theta\left[\frac{3}{2}\frac{\Delta\sigma'_{ij}}{2}\frac{\Delta\sigma'_{ij}}{2}\right]^{0.5}+(1-\theta)\Delta\sigma_1$$ Multiaxial term

$$U=\frac{1}{1-R}$$ Mean stress term

LC Growth

$$\left(\frac{da}{dN}\right)_{LC}=A(T-T_0) \quad \text{for} \quad T_0<T<T_A$$

$$\left(\frac{da}{dN}\right)_{LC}=BT^{\beta} \quad \text{for} \quad T_A<T<T_C$$

$a_i \geq 250\,\mu\text{m}$, or

$$\frac{da}{dN}=\max\left[\left(\frac{da}{dN}\right)_{MSC/PSC},\left(\frac{da}{dN}\right)_{LC}\right]$$

McDowell, et al., 2003

Conclusions

- DMA testing was performed to investigate the viscoelastic properties and transition temperatures
- Material exhibited time and temperature dependence
- Debonding of calcium carbonate particles and aluminosilicate agglomerates on the order of 50 to 200 μm lead to specimen failure for monotonic loading and initiated fatigue cracks under fatigue loading
- The ISV model captures both loading and unloading as well as rate dependence

Conclusions

- The MSF model equations need to be extended to elastomeric materials as well as calibrated and validated on SBR
- Fatigue experiments need to be conducted at lower strain amplitudes to investigate the high cycle fatigue response of the material

Acknowledgements

- The Center for Advanced Vehicular Systems (CAVS) at Mississippi State University (MSU)
- TARDEC
- Bill Bradford (TARDEC)
- Dr. Dave Ostberg (TARDEC)
- Dr. J. Brian Jordan (CAVS)
- Katherine Gilbert (CAVS)
- Savannah Ponder (CAVS)

This material is based upon work supported by the U.S. Army TACOM Life Cycle Command under Contract No. W56HZV-08-C-0236, through a subcontract with Mississippi State University, and was performed for the Simulation Based Reliability and Safety (SimBRS) research program.

Any opinions, findings and conclusions or recommendations expressed in this material are those of the author(s) and do not necessarily reflect the views of the U.S. Army TACOM Life Cycle Command.